

Online Supplemental Material (OSM) 3: Petrographic description of pottery thin-sections

Dirk Seidensticker

February 4, 2025

The mineralogical composition of 27 samples was studied using thin-sections petrography. Petrographic analysis was conducted using a Olympus BX41 microscope. Description and interpretation of observations was based on established reference works regarding ceramic petrography (MacKenzie et al., 2017; Quinn, 2022) and Stoops (2021). C/f-related distribution patterns are applied to all component of the coarse fraction. The descriptions are sorted chronologically, from the oldest to the youngest and in reference to the samples stratigraphic context as denoted in their original label. The identification of the corresponding thin-section is given as a label, consisting of the lower case site code and a running numbering of the general thin-section archive of the first-authors project separated by a hashtag (Tab. 1).

Contents

1	Pikunda	3
1.1	PIK 87/1-1:35 (pik#11; Mandombe style; Fig. 3M–N)	3
1.2	PIK 87/1-2:70 (pik#55; Ebambe style; Fig. 3A–C)	4
1.3	PIK 87/1-2:123 (pik#10; Mandombe style)	5
1.4	PIK 87/1-7:12 (pik#4; Fig. S7.3; Pikunda-Munda style; Seidensticker, 2021, 427 Pl. 46.21)	6
1.5	PIK 87/1-8:1 (pik#5; Fig. S7.6; cf. Ngbanja style; Seidensticker, 2021, 428 Pl. 47.20)	7
1.6	PIK 87/1-8:2 (pik#56; Fig. S7.7; cf. Ngbanja style; Seidensticker, 2021, 428 Pl. 47.21)	8
1.7	PIK 87/1-9:5 (pik#54; Fig. S7.4; Pikunda-Munda style; Seidensticker, 2021, 428 Pl. 47.7)	9
1.8	PIK 87/1-9:7 (pik#6; Fig. S7.8; cf. Ngbanja style; Seidensticker, 2021, 428 Pl. 47.19)	10
1.9	PIK 87/1-12:1 (pik#53; Fig. S7.2; Lusako style; Seidensticker, 2021, 426 Pl. 45.16)	11
1.10	PIK 87/2-1:40 (pik#99; Fig. S7.12; Ebambe style; Seidensticker, 2021, 430 Pl. 49.10)	12
1.11	PIK 87/2-4:73 (pik#98; Fig. S7.5; Pikunda-Munda style; Seidensticker, 2021, 429 Pl. 48.25)	13
1.12	PIK 87/2-6:52 (pik#97; Fig. S7.11; cf. modern; Seidensticker, 2021, 430 Pl. 49.5)	14
1.13	PIK 87/2-6:77 (pik#9)	15
1.14	PIK 87/501:4 (pik#57; Fig. 3O)	16
2	Munda	17
2.1	MUN 87/2-1-1-2:2 (mun#3; Fig. S9.1; Pikunda-Munda style; Seidensticker, 2021, 472 Pl. 91.2)	17
2.2	MUN 87/2-1-1-4:2 (mun#2; Fig. S9.2; Pikunda-Munda style; Seidensticker, 2021, 472 Pl. 91.1)	18
2.3	MUN 87/2-1-1-5:2 (mun#104; Fig. S9.3; Pikunda-Munda style; Seidensticker, 2021, 472 Pl. 91.5)	19
2.4	MUN 87/2-1-1-7:2 (mun#105; Fig. S9.6; Pikunda-Munda style; Seidensticker, 2021, 472 Pl. 91.6)	20
2.5	MUN 87/2-1-1-8:1 (mun#106; Fig. S9.5; Pikunda-Munda style; Seidensticker, 2021, 472 Pl. 91.8)	21
2.6	MUN 87/2-1-1-8:3 (mun#107; Fig. S9.4; Pikunda-Munda style; Seidensticker, 2021, 472 Pl. 91.7)	22

2.7 MUN 87/2-1-3-1:2 (mun#103; Fig. S9.7; Pikunda-Munda style; Seidensticker, 2021, 473 Pl. 92.2)	23
2.8 MUN 87/2-1-3-4:4 (mun#100; Fig. S9.8; Pikunda-Munda style; Seidensticker, 2021, 473 Pl. 92.4)	24
2.9 MUN 87/2-1-3:3 (mun#102; Fig. S9.9; Pikunda-Munda style; Seidensticker, 2021, 473 Pl. 92.5)	25
2.10 MUN 87/2-1-3:7 (mun#101; Fig. S9.10; Pikunda-Munda style; Seidensticker, 2021, 474 Pl. 93.1)	26
2.11 MUN 87/1-0-2-1:1 (mun#109; Fig. S9.12; Ebambe style; Seidensticker, 2021, 470 Pl. 89.4)	27
2.12 MUN 87/1-0-2-4:2 (mun#110; Fig. S9.11; Ebambe style; Seidensticker, 2021, 470 Pl. 89.2)	28
2.13 MUN 87/1-0-2-6:1 (mun#17; Fig. S9.14; Ebambe style; Seidensticker, 2021, 471 Pl. 90.2)	29
2.14 MUN 87/1-0-2-6:2 (mun#108; Fig. S9.13; Ebambe style; Seidensticker, 2021, 471 Pl. 90.1)	30
3 Wafanya	31
3.1 WAF 83/16-2:1 (waf#47; Fig. S12.2; Monkoto style; Wotzka, 1995, 504 Pl. 70.10) .	31
3.2 WAF 83/16-2:3 (waf#48; Fig. S12.6; 3K–L; Bekongo style; Wotzka, 1995, 503 Pl. 69.6) .	32
3.3 WAF 83/16-5:33 (waf#96; Fig. S12.5; Bekongo style; Wotzka, 1995, 503 Pl. 69.5) .	33
3.4 WAF 83/16-7-1:2 (waf#49; Fig. S12.7; Longa style; Wotzka, 1995, 503 Pl. 69.9) .	34
4 Salonga National Park	35
4.1 SNP 01 7:1 (snp#43; Fig. S11.1; cf. Bokuma style)	35
4.2 SNP 03-4:1 (snp#42; Fig. 3G–H; S11.5)	36
4.3 SNP 03-4:4 (snp#45)	37
4.4 SNP 03-4:5 (snp#46; Fig. 3E–F)	38
4.5 SNP 03-7:1 (snp#44; Fig. 3I; S11.7)	39
5 Monkoto	40
5.1 MON 83/101:1 (mon#50; Fig. S12.1; Monkoto style; Wotzka, 1995, 506 Pl. 72.5) .	40
5.2 MON 83/101:3 (mon#51; Fig. S12.3; 3D; Monkoto style; Wotzka, 1995, 506 Pl. 72.6) .	41
5.3 MON 83/101:4 (mon#52; Fig. S12.4; 3J; Wotzka, 1995, 505 Pl. 71.6)	42

1 Pikunda

1.1 PIK 87/1-1:35 (pik#11; Mandombe style; Fig. 3M–N)

The sample shows a homogeneous non-calcareous fine fraction (orange-brown & reddish towards the inner/outer wall [PPL]) with stipple speckled b-fabric (localized monostriation). Voids are very narrow and usually oriented wall-parallel with respect to the plane of the section. The coarse fractions is dominated by sub-rounded quartz and sub-rounded

iron rich heterogeneous clay pellets (dark brown [PPL]) in a bimodal grain-size distribution. Also common is muscovite, showing a tendency towards wall-parallel orientation. Rare are zircon, staurolite, tourmaline, plagioclase, carbonized plant matter and isolated sponge-spicules. The c/f-related distribution pattern is single-spaced porphyric.

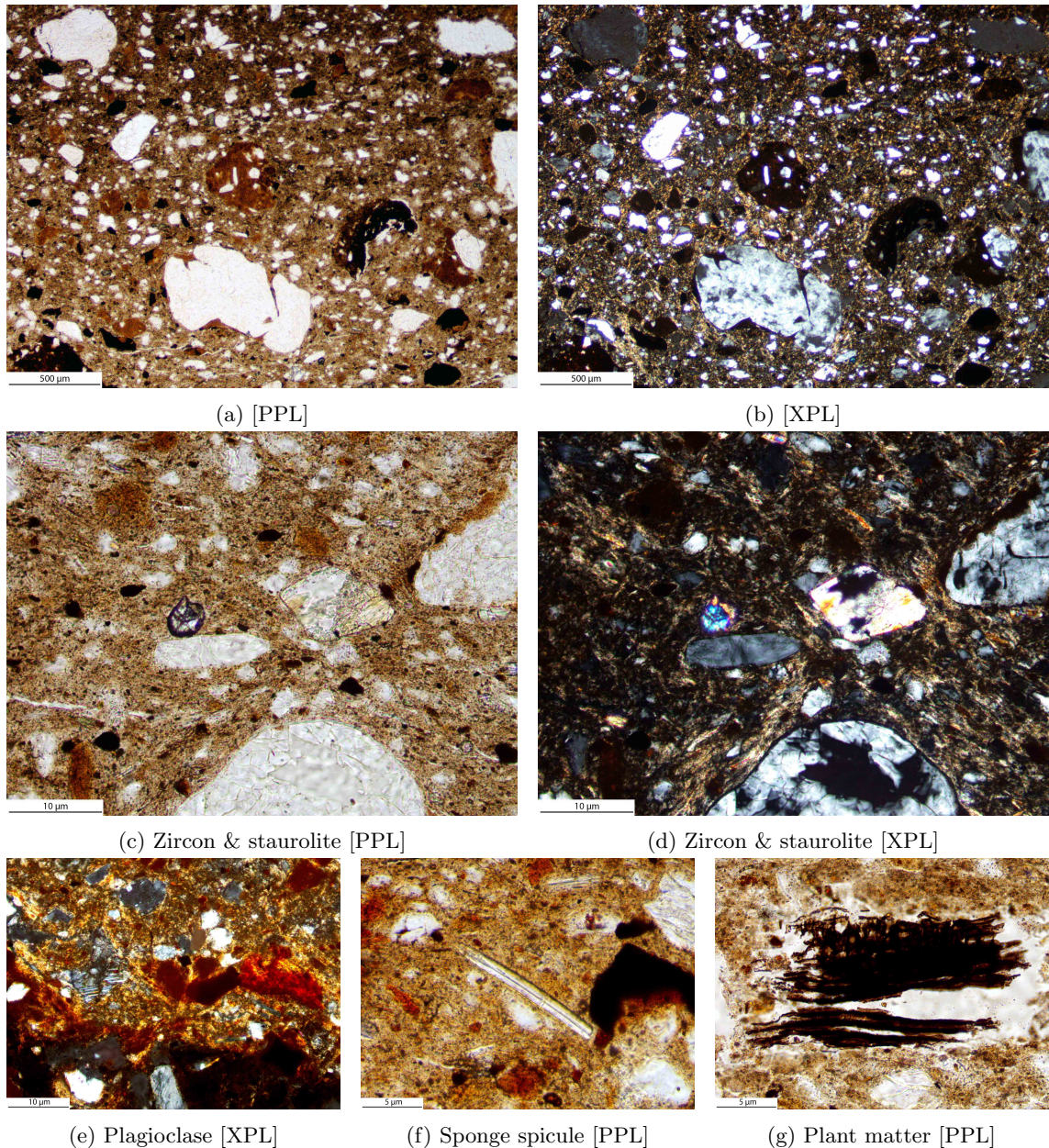


Figure S13

1.2 PIK 87/1-2:70 (pik#55; Ebambe style; Fig. 3A–C)

The fine fraction is homogeneous and non-calcareous (light yellowish [PPL]) with unistriated b-fabric. The section shows nearly no or very narrow voids. The dominant component of the coarse fraction are sponge spicules, mostly cut longitudinal and oriented wall-parallel in relation to the plane of the section, and a very

fine (sub-)angular quartz fraction. Rare are sub-angular homogeneous clay pellets, muscovite, tourmaline, and zircon. The c/f-related distribution pattern is single-spaced porphyric (open porphyric if only quartz grains are regarded as coarse material).

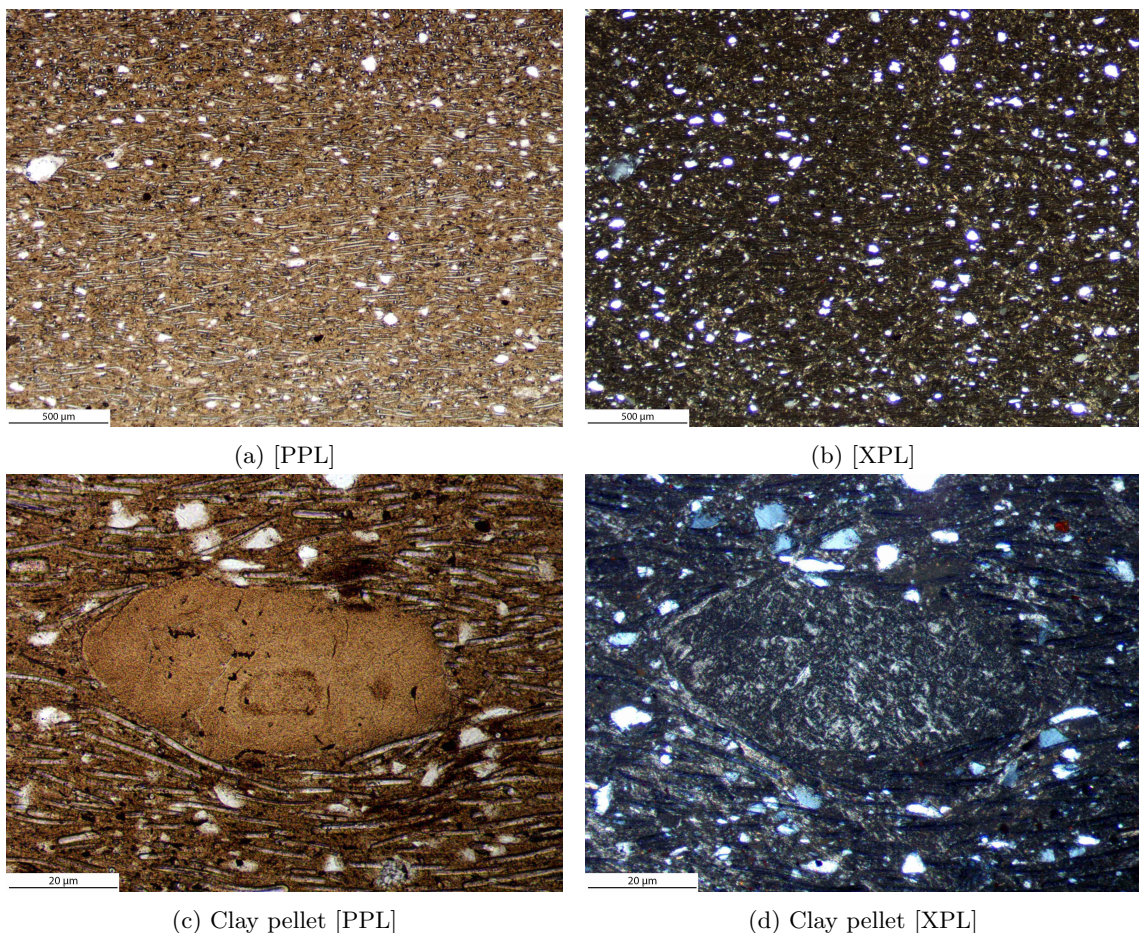


Figure S14

1.3 PIK 87/1-2:123 (pik#10; Mandombe style)

The fine fraction is homogeneous and non-calcareous (light yellowish to dark brown [PPL]) with stipple speckled b-fabric. Voids show no orientation. The coarse-fraction consists mainly of sub-angular quartz in clear bimodal grain-size distribution, including a high proportion of

runiquartz. Common are sub-rounded iron rich (dark reddish [PPL]) heterogeneous clay pellets. Occasionally present are muscovite and biotite as well as charred plant matter, plagioclase and zircon. The c/f-related distribution pattern is single-spaced porphyric.

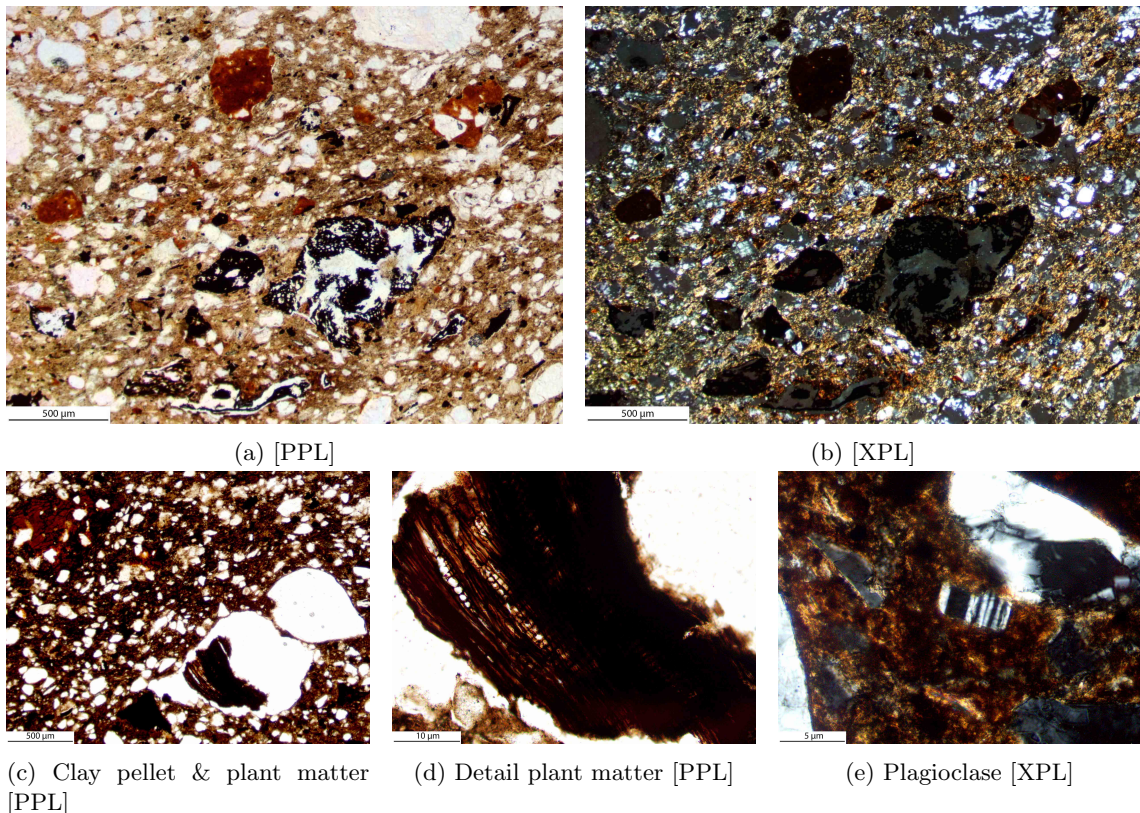


Figure S15

1.4 PIK 87/1-7:12 (pik#4; Fig. S7.3; Pikunda-Munda style; Seidensticker, 2021, 427 Pl. 46.21)

The samples fine fraction (light yellowish to dark brown [PPL]) is heterogeneous and non-calcareous with stipple-speckled b-fabric. Voids are rare or very narrow, without any discernible orientation. The main component of the coarse fraction are sponge spicules. These are mostly cut transverse and lesser longitudinal in relation to the plane of the section. Also dominant

part of the coarse fraction is fine quartz in an unimodal grain-size distribution. Occasionally, the larger fraction of quartz particles consists of runiquartz or rock fragments (sandstone) (e). To a lesser degree present are biotite and muscovite as well as plagioclases (f), kyanite (c-d) and zircon. The c/f-related distribution pattern is single-spaced porphyric.

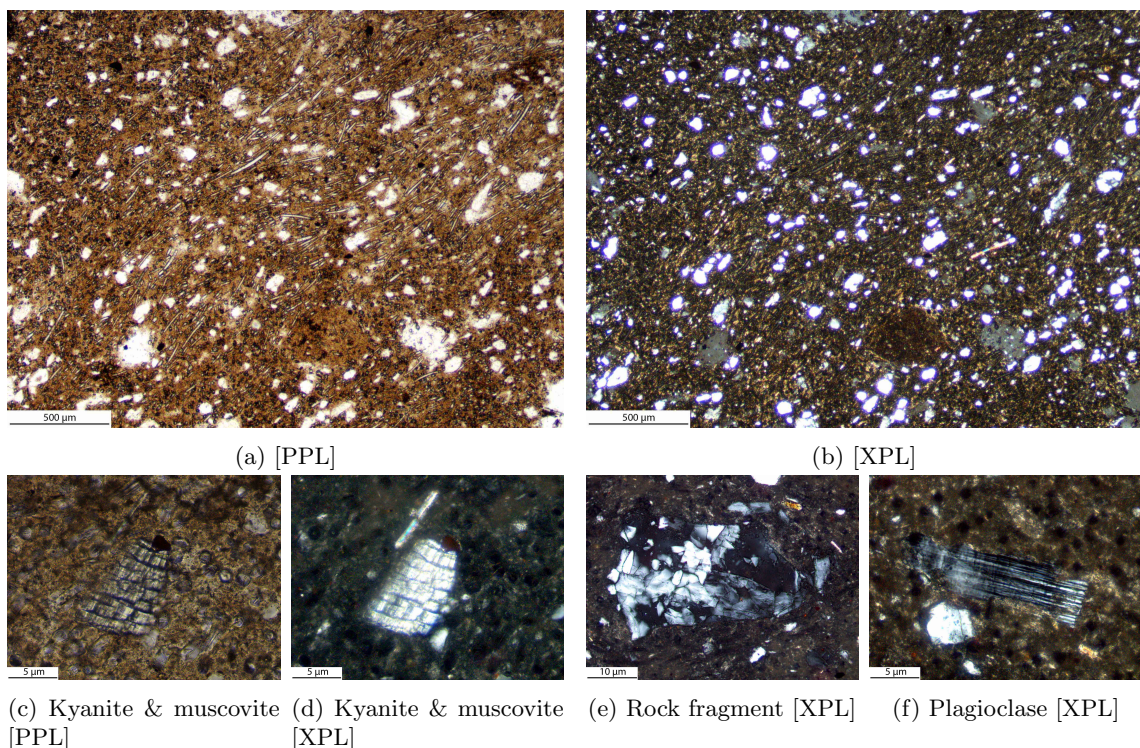


Figure S16

1.5 PIK 87/1-8:1 (pik#5; Fig. S7.6; cf. Ngbanja style; Seidensticker, 2021, 428 Pl. 47.20)

The section shows a homogeneous non-calcareous, iron-rich fine fraction (dark brown [PPL]) with undifferentiated b-fabric. Secondary calcite is visible on all pores and around the elements of the coarse fraction. Voids are – relative to the plane of the section – oriented U-shaped in one part and wall-parallel in the other.

This is regarded as indication for a shaping via coiling. The coarse fractions is characterized by sub-angular quartz in a bimodal grain-size distribution. Also present is muscovite and occasionally zircon (c-d). The c/f-related distribution pattern is single-spaced porphyric.

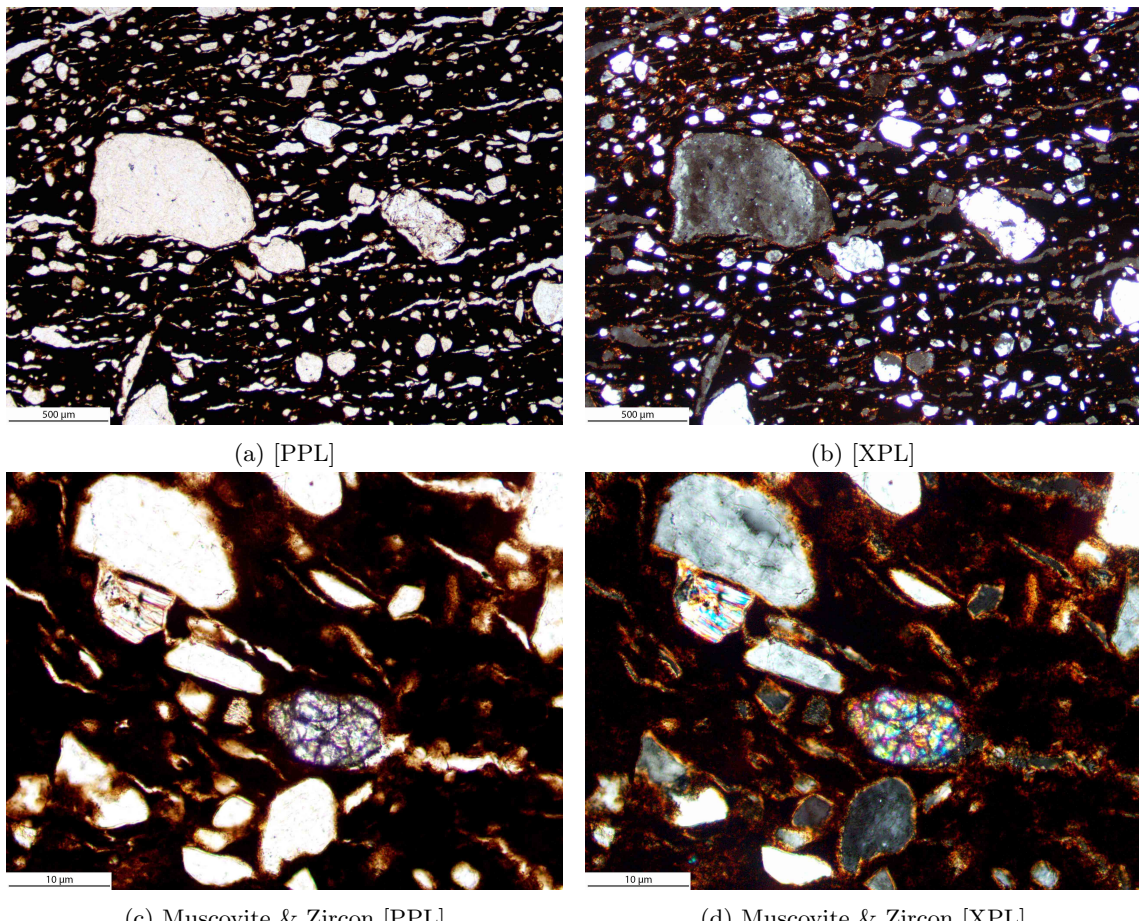


Figure S17

1.6 PIK 87/1-8:2 (pik#56; Fig. S7.7; cf. Ngbanja style; Seidensticker, 2021, 428 Pl. 47.21)

The fine fraction is homogeneous, non-calcareous, and slightly iron rich (reddish-brown [PPL]) with undifferentiated to slightly stipple-speckled b-fabrics. Voids are very narrow and oriented diagonally in relation to the plane of the section; similar as the coarse fraction. The dominant component of the coarse-fractions is densely packed, unimodally sorted, angular to

sub-angular quartz. Some quartz grains shows rolling extinction (b), indicating metamorphic degradation. Some of the larger constituents of the coarse fraction are rock fragments (sandstone) (c-d). Occasionally present are muscovite, biotite, tourmaline, staurolite, and zircon. The c/f-related distribution pattern is single-spaced porphyric.

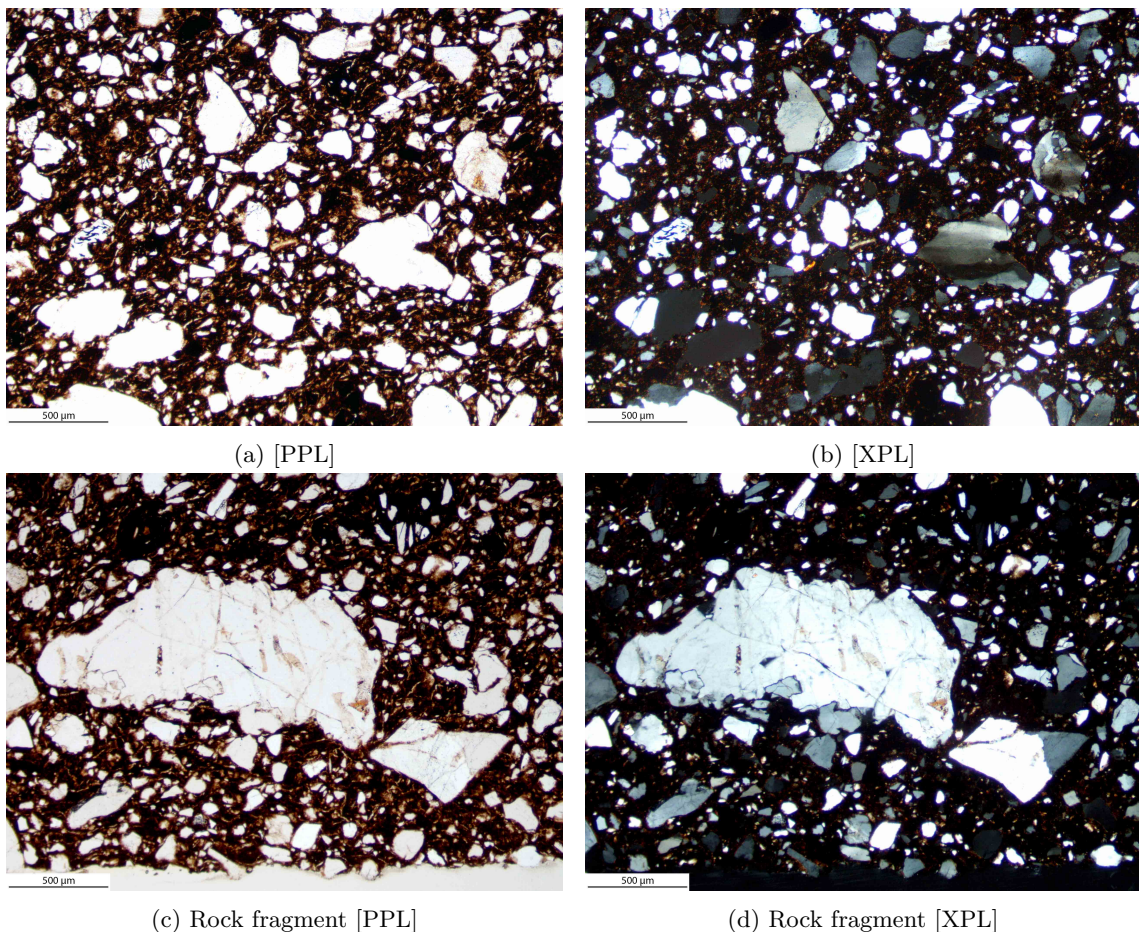


Figure S18

1.7 PIK 87/1-9:5 (pik#54; Fig. S7.4; Pikunda-Munda style; Seidensticker, 2021, 428 Pl. 47.7)

The samples fine fraction (light yellow, reddish brown and dark brown [PPL]) is heterogeneous and non-calcareous with stipple-speckled b-fabric. Voids are more pronounced towards the inside of the sherd and generally wall-parallel in relation to the plane of the section. The

coarse fraction is dominated by densely packed sponge spicules, mostly transversely cut, and fine sub-angular quartz appearing in a unimodal grain-size distribution. Muscovite and zircon are occasionally present. The c/f-related distribution pattern is single-spaced porphyric.

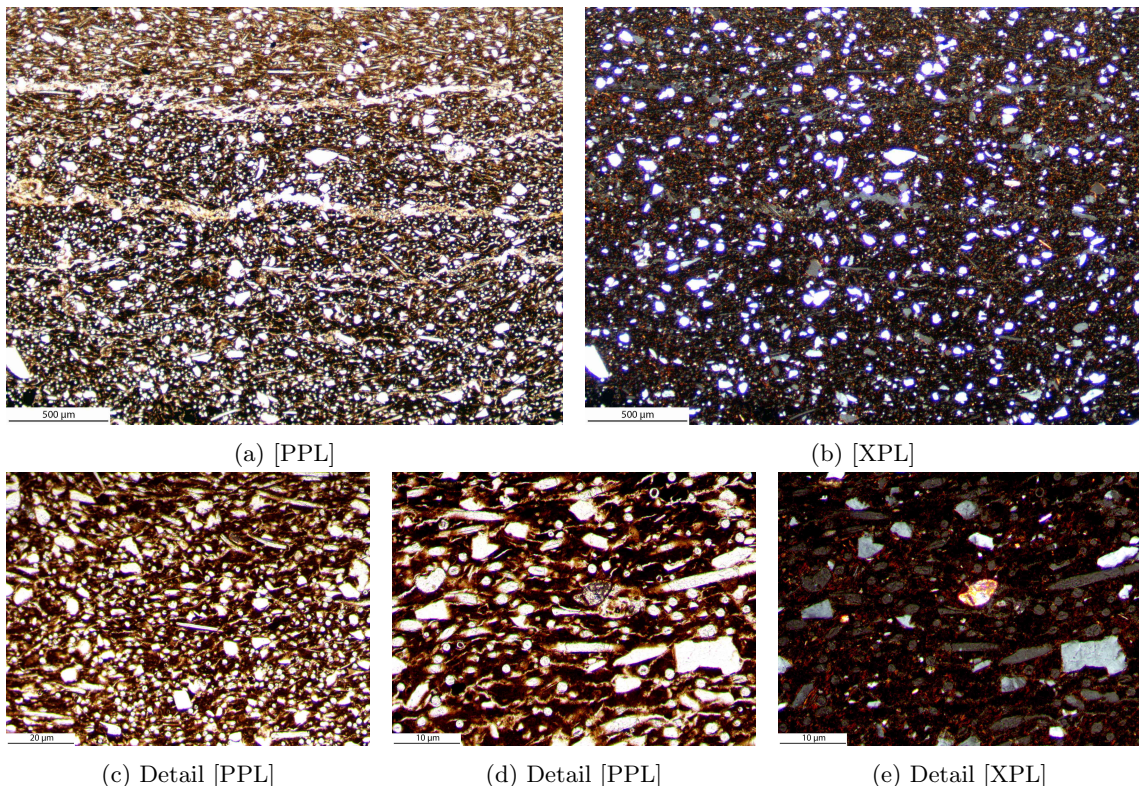


Figure S19

1.8 PIK 87/1-9:7 (pik#6; Fig. S7.8; cf. Ngbanja style; Seidensticker, 2021, 428 Pl. 47.19)

The fine fraction (yellowish to reddish-brown [PPL]) is homogeneous, non-calcareous with stipple-speckled b-fabric. Voids are numerous but narrow and organized in a diagonal (S) configuration in respect to the plane of the section. The coarse fraction is dominated by angular quartz and rock fragments (sandstone) in a bi-

modal grain-size distribution. The quartz fraction is partially comprised of runiquartz. Also common are dark-brown to opaque (PPL) iron-rich inclusions (soil deposits). Rarely present are muscovite and biotite. The c/f-related distribution pattern is single-spaced porphyric.

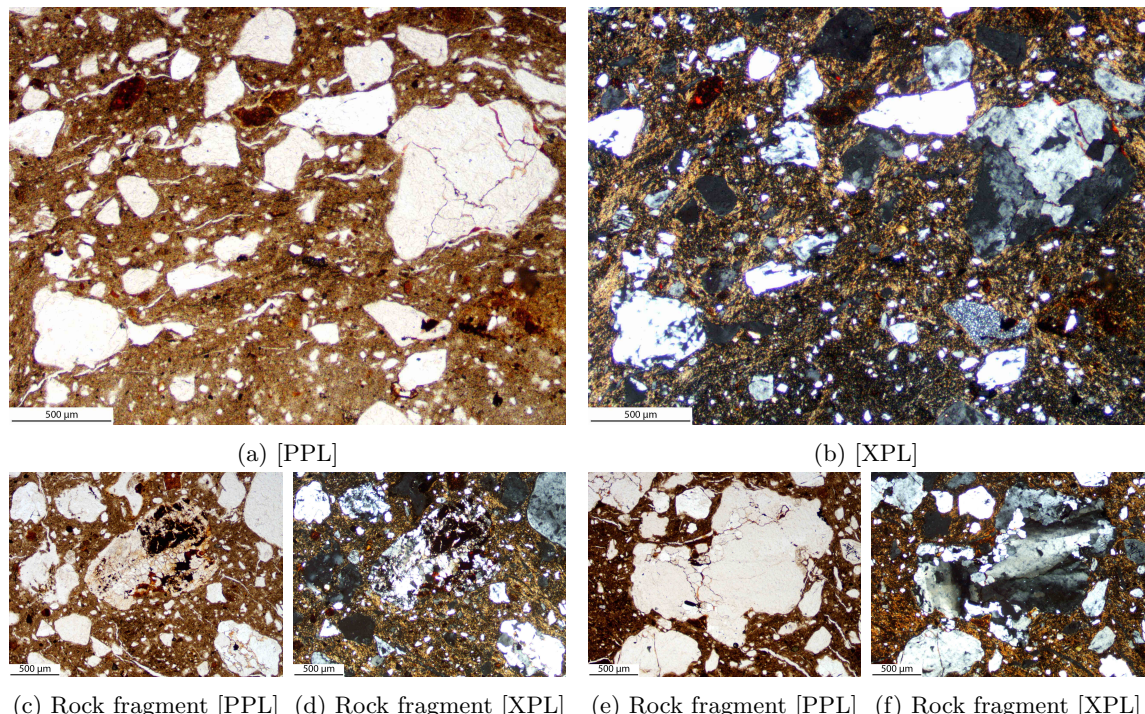


Figure S20

1.9 PIK 87/1-12:1 (pik#53; Fig. S7.2; Lusako style; Seidensticker, 2021, 426 Pl. 45.16)

The fine fraction is homogeneous and non-calcareous (reddish brown [PPL]) with undifferentiated b-fabric. Voids are rare, rounded, and in a diagonal (Z) configuration. The coarse fraction is dominated by densely packed sponge spicules (single spaced porphyric), mostly trans-

versely cut in respect to the plane of the section, and sub-angular quartz. The quartz fraction is also shows diagonal orientations. Muscovite, biotite and tourmaline is very rarely present. The c/f-related distribution pattern is single- to double-spaced porphyric.

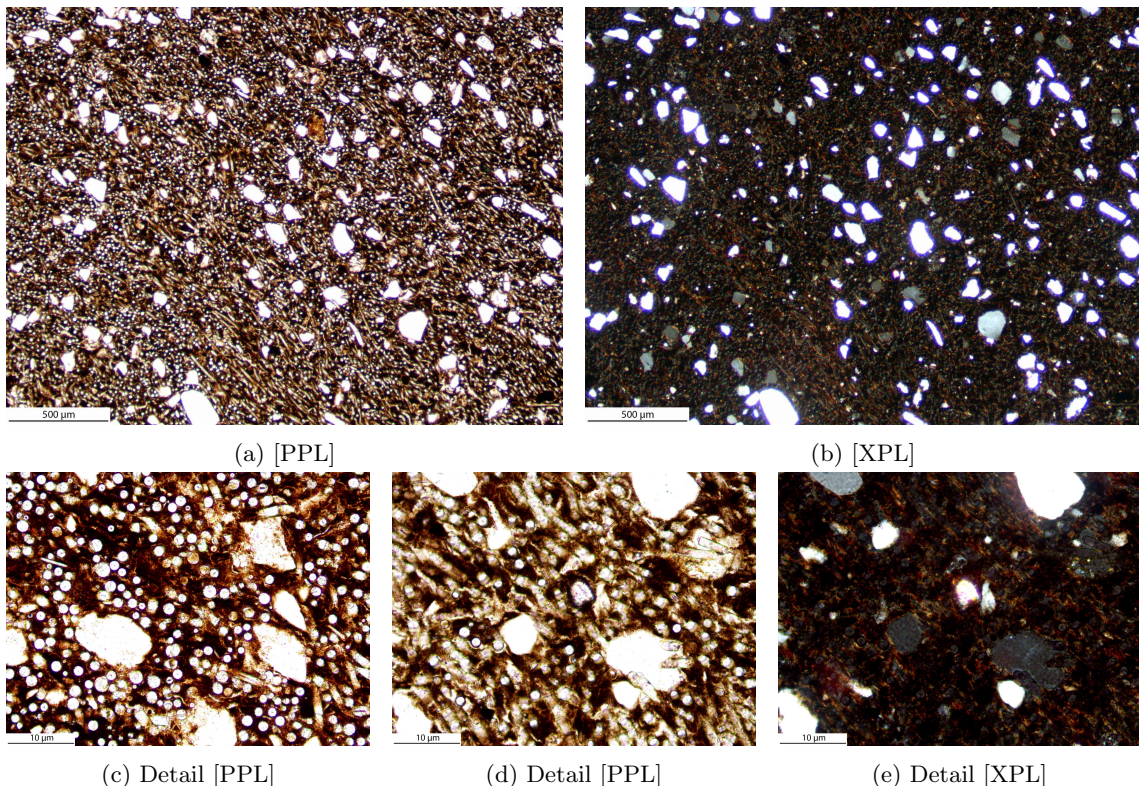


Figure S21

1.10 PIK 87/2-1:40 (pik#99; Fig. S7.12; Ebambe style; Seidensticker, 2021, 430 Pl. 49.10)

The sample shows a homogeneous, non-calcareous fine fraction (reddish brown [PPL]) with undifferentiated b-fabric. Voids are predominantly oriented wall-parallel with respect to the plane of the section. The main constituent of the coarse fraction are densely packed sponge spicules that are mostly cut transversely.

Also very common is sub-angular quartz. Also present is charred organic matter (c–e). Rarely present is muscovite. The c/f-related distribution pattern is single-spaced porphyric (double-spaced to open porphyric if only quartz grains are regarded as coarse material).

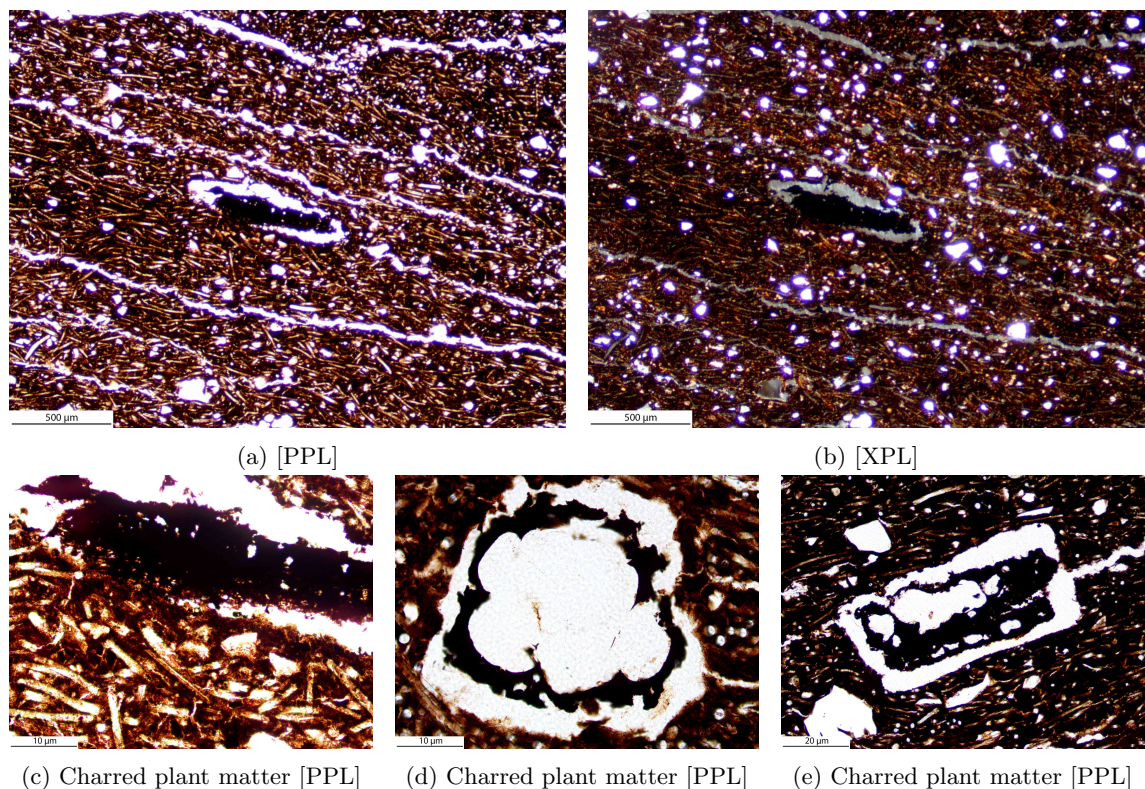


Figure S22

1.11 PIK 87/2-4:73 (pik#98; Fig. S7.5; Pikunda-Munda style; Seidensticker, 2021, 429 Pl. 48.25)

The samples fine fraction is homogeneous and non-calcareous (yellowish-orange brown [PPL]) with undifferentiated b-fabric. Voids are very rare. The coarse fraction is defined by sponge spicules, often cut transversely in respect to the plane of the section. Also a common part of the coarse fraction is sub-angular quartz. The quartz fraction shows a bimodal grain-size distri-

bution. Some of the larger quartz grains shows rolling extinction (e). Occasionally present are charred plant matter (c), muscovite and tourmaline. The c/f-related distribution pattern is single-spaced porphyric (single- to double-spaced porphyric if only quartz grains are regarded as coarse material).

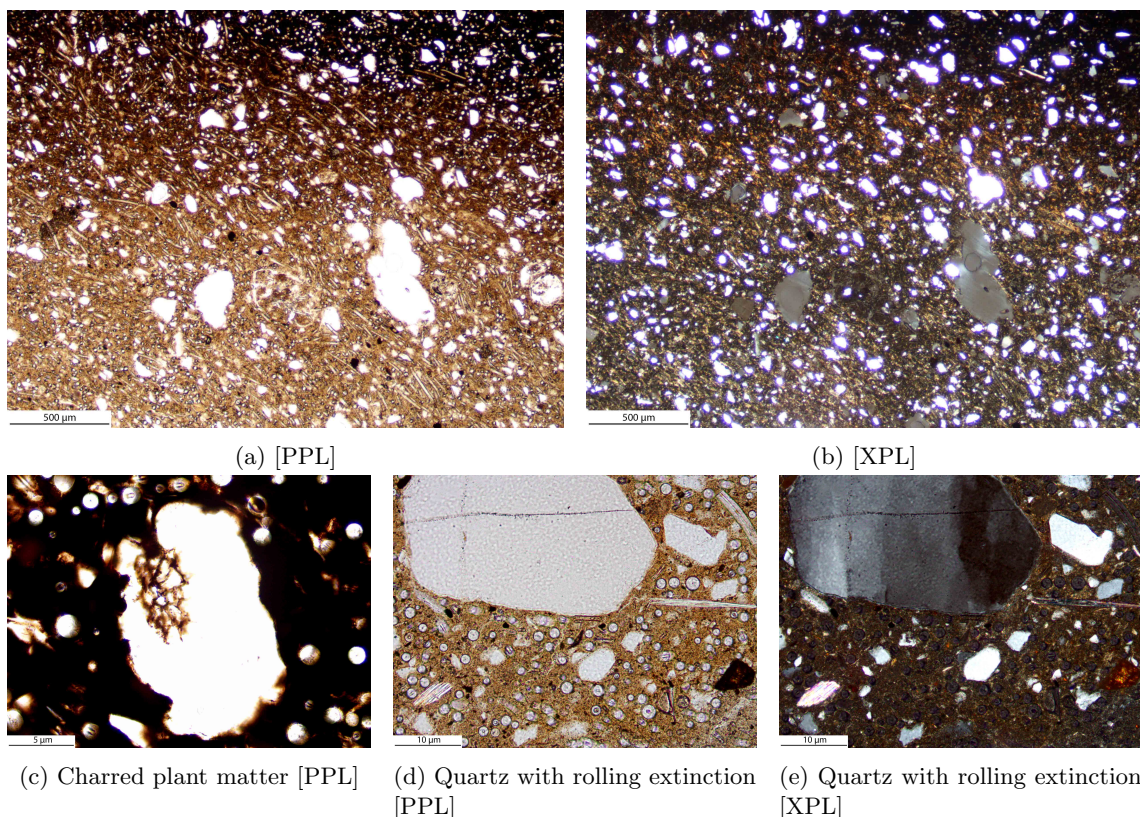


Figure S23

1.12 PIK 87/2-6:52 (pik#97; Fig. S7.11; cf. modern; Seidensticker, 2021, 430 Pl. 49.5)

The fine fraction is homogeneous and non-calcareous (brown [PPL]) with stipple-speckled b-fabric. The narrow, but common voids run predominantly diagonally, in reference to the plane of the section, through the sample. The main constituent of the coarse fraction is sub-rounded quartz in an unimodal grain-size dis-

tribution. Some of the larger grains can be identified as rock fragments (sandstone). The quartz fraction is partially comprised of rumi-quartz. Occasionally present is staurolite. Exceptional is a small piece of slag showing distinct prismatic fayalite crystals (e). The c/f-related distribution pattern is single-spaced porphyric.

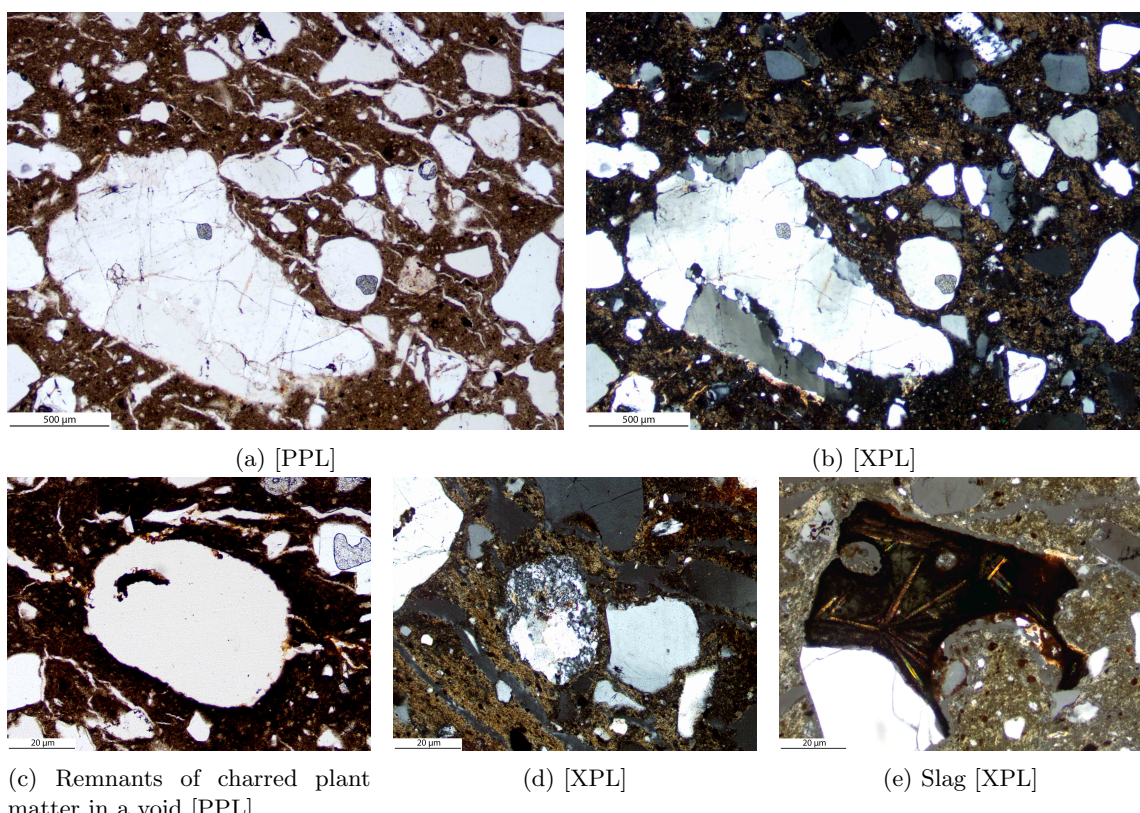


Figure S24

1.13 PIK 87/2-6:77 (pik#9)

The samples fine fraction (light yellow to reddish brown [PPL]) is homogeneous and non-calcareous with stipple-speckled b-fabric. The color at the inside is considerably more reddish [PPL]. Voids are not very numerous, but generally in a diagonal (Z) configuration in respect to the plane of the section. The dominant component of the coarse fraction is densely packed sub-

angular quartz in a unimodal grain-size distribution. The quartz fraction is partially comprised of runiquartz. Opaque iron-rich sub-angular inclusions are common. Heterogeneous iron-rich clay pellets (reddish brown [PPL]) and biotite are rare. The c/f-related distribution pattern is single-spaced porphyric.

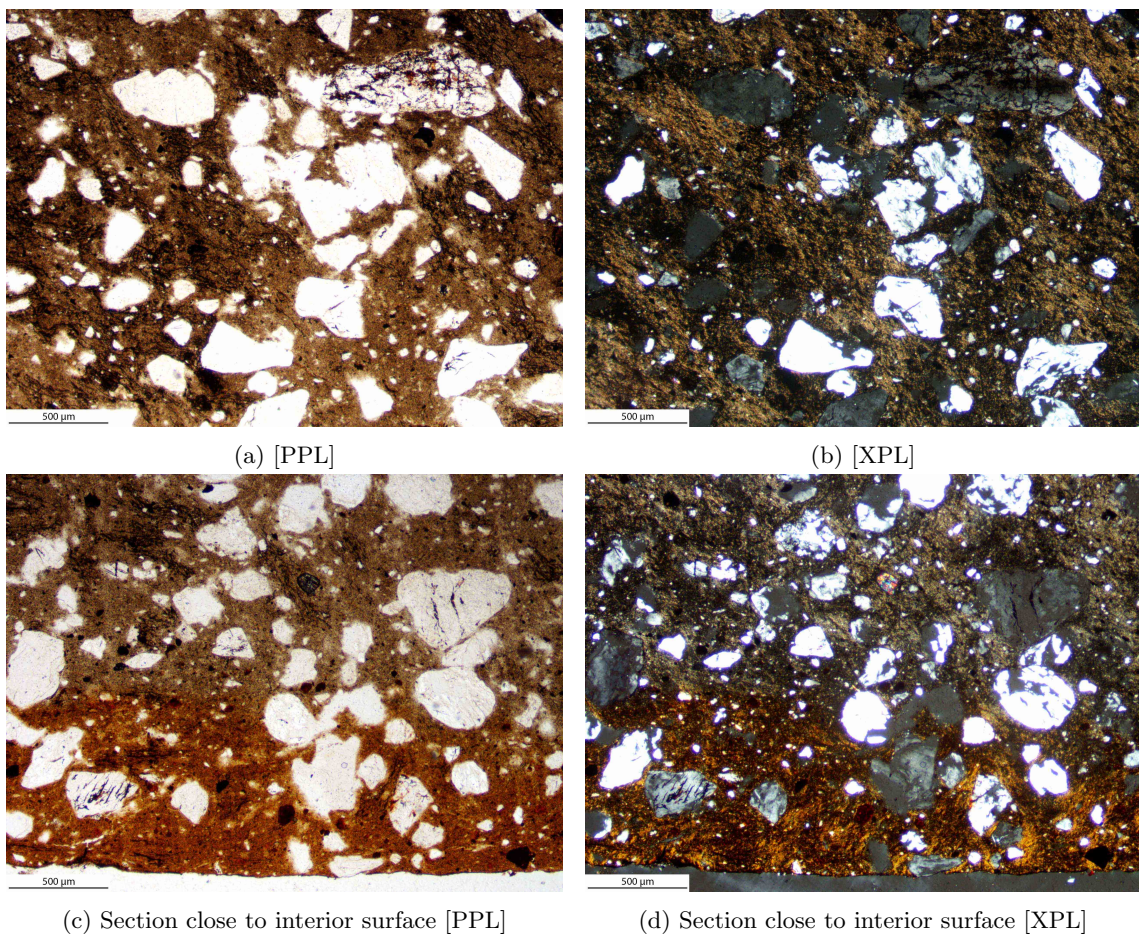


Figure S25

1.14 PIK 87/501:4 (pik#57; Fig. 3O)

The fine fraction is non-calcareous (beige to dark brown [PPL]) with stipple-speckled (localized uniserialiation). Voids are oriented crescent-shaped (U-shaped) in relation to the plane of the section. The coarse fraction is dominated by unimodally sorted sub-angular quartz and

rock fragments (sandstone). The quartz shows rolling extinction and a proportion is comprised of runiquartz. Staurolite and muscovite are occasionally present. The c/f-related distribution pattern is single-spaced porphyric.

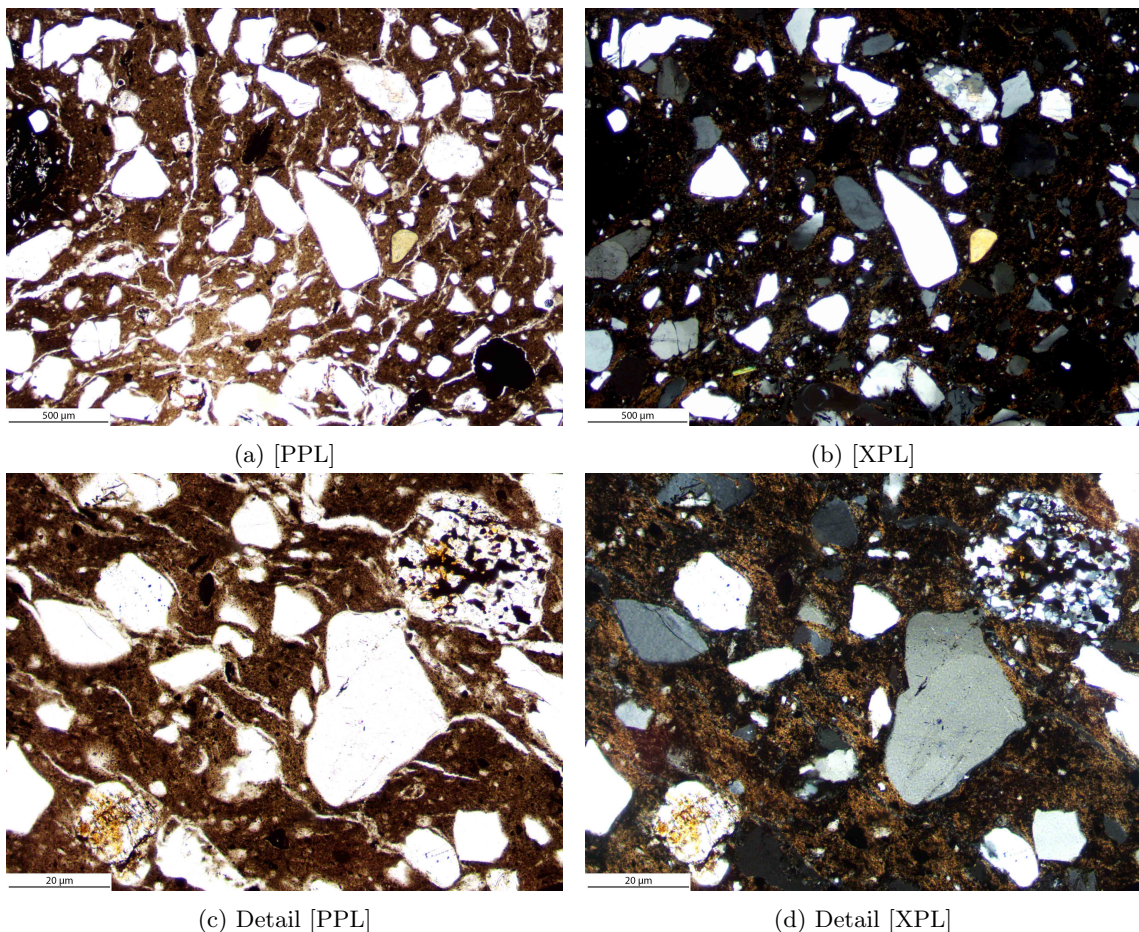


Figure S26

2 Munda

2.1 MUN 87/2-1-1-2:2 (mun#3; Fig. S9.1; Pikunda-Munda style; Seidensticker, 2021, 472 Pl. 91.2)

The sample shows a two-tiered non-calcareous fine fraction with a clear border between the two parts. The main body of the sherd with undifferentiated b-fabric (dark-reddish brown [PPL]), while especially the exterior part with stipple-speckled b-fabric (light yellowish [PPL]). Voids are very narrow to non-existent. The main component of the coarse fraction are sponge spicules. In the plane of the section, they ap-

pear equally cut transversal and longitudinal (c). Also a dominant part of the coarse fraction is fine, sub-angular quartz in a unimodal grain-size distribution. Rarely occurring is tourmaline (c-d). The c/f-related distribution pattern is single-spaced porphyric (double-spaced if open porphyric if only quartz grains are regarded as coarse material).

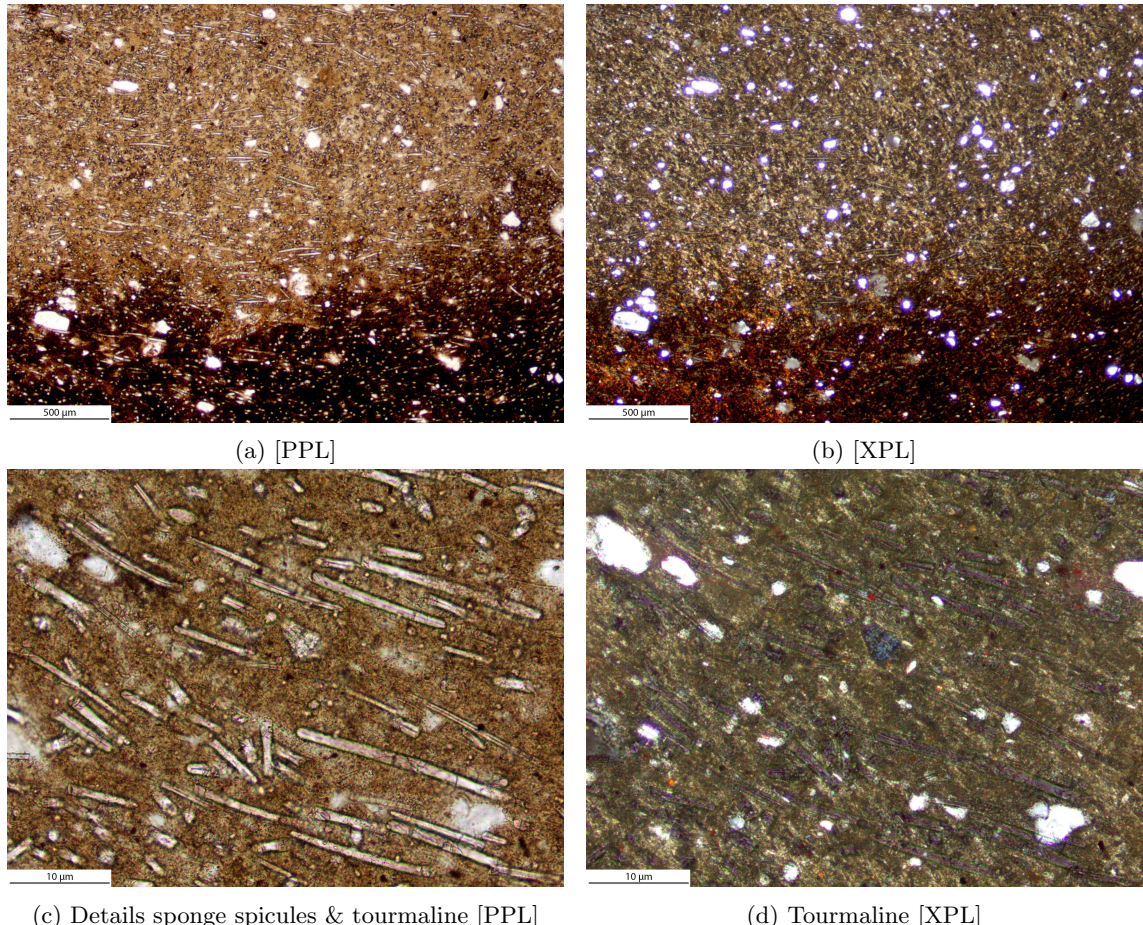


Figure S27

2.2 MUN 87/2-1-1-4:2 (mun#2; Fig. S9.2; Pikunda-Munda style; Seidensticker, 2021, 472 Pl. 91.1)

The samples two-tiered non-calcareous fine fraction shows a gradient between the two parts. The core with undifferentiated b-fabric (dark-brown [PPL]), while the exterior and interior parts with stipple-speckled b-fabric (light yellowish [PPL]). Voids are very narrow to non-existent. The main component of the coarse fraction are sponge spicules. The spicules are often cut longitudinal to the plane of the sec-

tion, with transversal cut spicules clustering in specific locations. The second dominant part of the coarse fraction is fine, sub-angular quartz in a unimodal grain-size distribution. Occasionally present is muscovite and very rare are staurolite, kyanite (c-d), and tourmaline (e). The c/f-related distribution pattern is single-spaced porphyric (double-spaced porphyric if only quartz grains are regarded as coarse material).

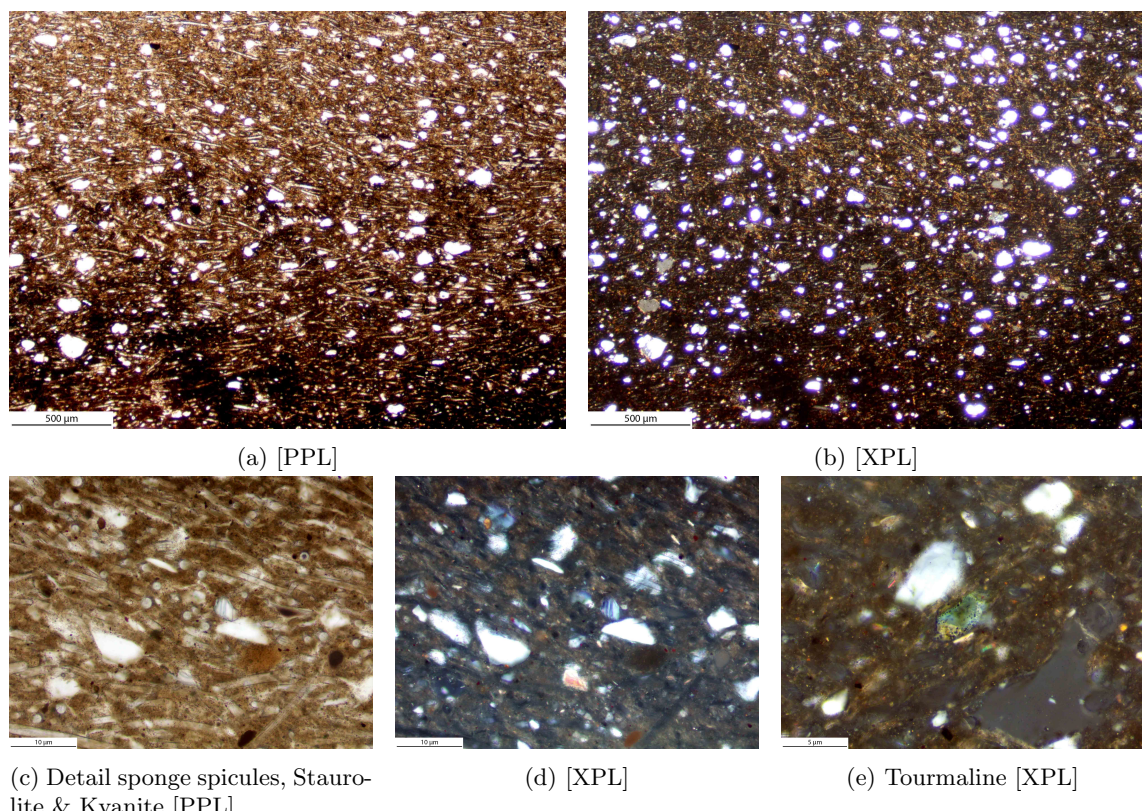


Figure S28

2.3 MUN 87/2-1-1-5:2 (mun#104; Fig. S9.3; Pikunda-Munda style; Seidensticker, 2021, 472 Pl. 91.5)

The samples fine fraction (darkish brown [PPL]) is homogeneous and non-calcareous with undifferentiated b-fabric. There are only very narrow voids visible, which show no apparent orientation. The coarse fraction is dominated by sponge spicules and sub-angular quartz in a unimodal grain-size distribution. The sponge spicules are

predominantly cut transversal to the plane of the section (c). Occasionally present are clay pellets (a–b) and charred organic matter (d–e). Rarely present are muscovite and staurolite. The c/f-related distribution pattern is single-spaced porphyric (double-spaced to open porphyric if only quartz grains are regarded as coarse material).

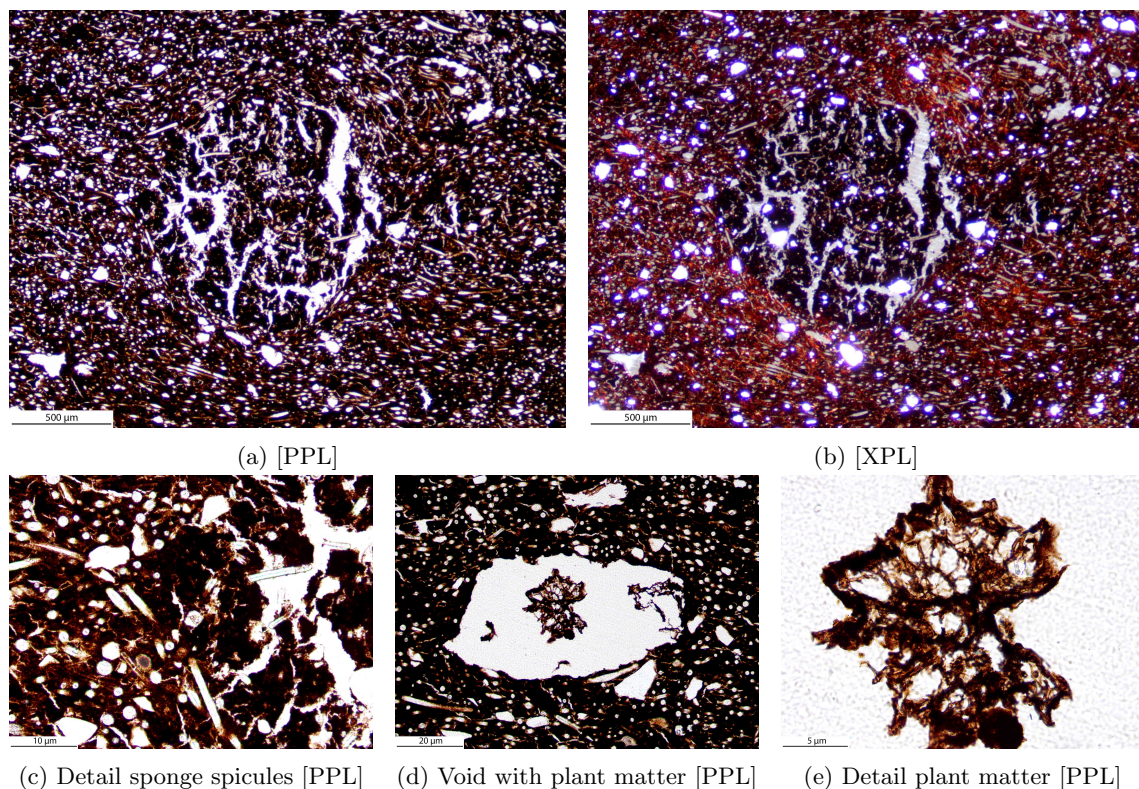


Figure S29

2.4 MUN 87/2-1-1-7:2 (mun#105; Fig. S9.6; Pikunda-Munda style; Seidensticker, 2021, 472 Pl. 91.6)

The sample shows a homogeneous non-calcareous fine fraction (darkish brown [PPL]) with undifferentiated b-fabric. Voids are rare and only very narrow. The coarse fraction is dominated by sponge spicules whose orientation in regard to the plane of the section is heterogeneous: there are zones in which the spicules are predominantly cut longitudinal, while in other zones spicules are predominantly cut transver-

sal. There is no clear pattern in regard to the organization of these zones. The second-tier component of the coarse fraction is sub-angular quartz in a unimodal grain-size distribution. Occasionally present are clay pellets (c-d). Muscovite is only rarely present. The c/f-related distribution pattern is single-spaced porphyric (double-spaced to open porphyric if only quartz grains are regarded as coarse material).

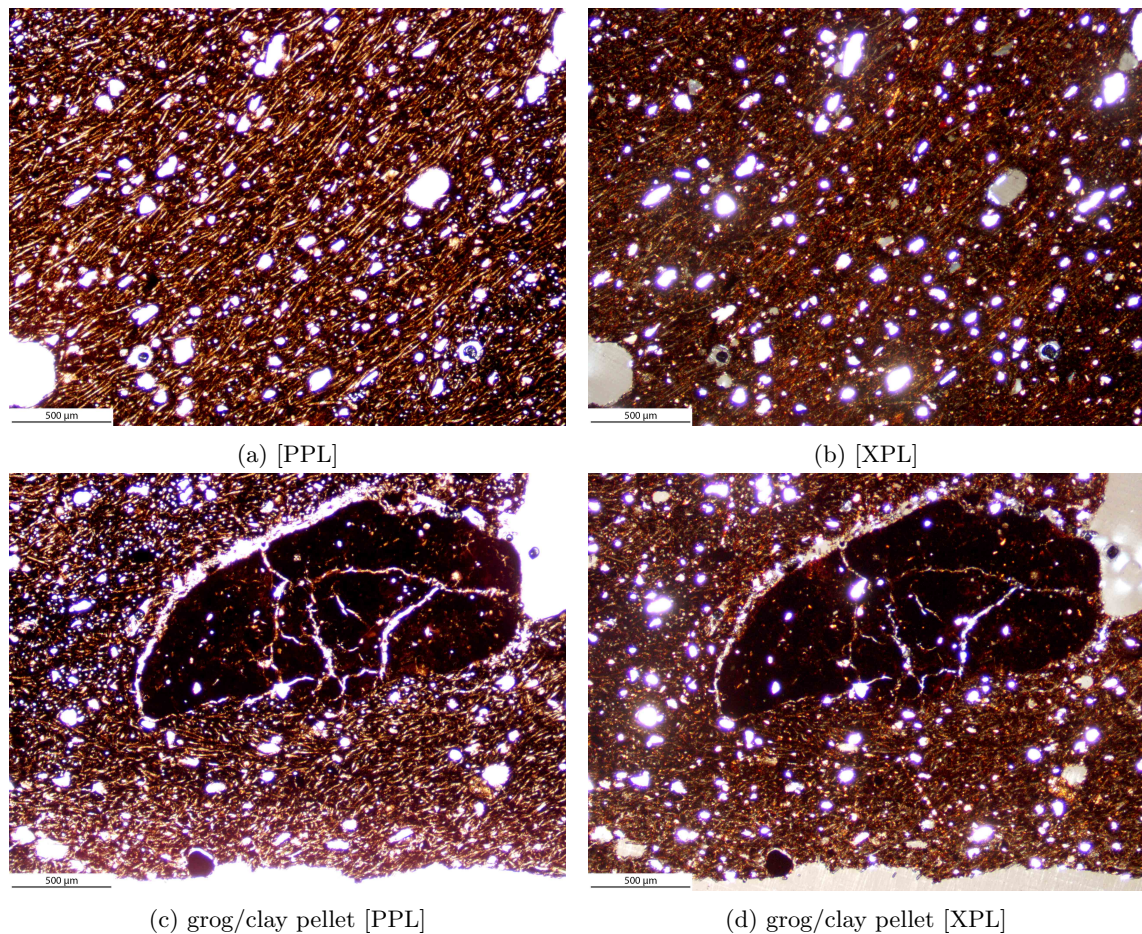


Figure S30

2.5 MUN 87/2-1-1-8:1 (mun#106; Fig. S9.5; Pikunda-Munda style; Seidensticker, 2021, 472 Pl. 91.8)

The sections non-calcareous fine fraction is two-tiered: the main body with undifferentiated b-fabric (very darkish brown [PPL]), while the exterior part with stipple-speckled b-fabric (reddish brown [PPL]). The boundary between the two zones is slightly blurry (a–b). Voids are only rarely present and in case they are present very narrow. The main components of the coarse

fraction are sponge spicules, showing no predominant organization with spicules cut transversal or longitudinal to the plane of the section equally. Also dominating is angular quartz in a unimodal grain-size distribution. Rare are clay pellets (a–b), charred organics, muscovite, microcline (c–d) and kyanite (e). The c/f-related distribution pattern is single-spaced porphyric.

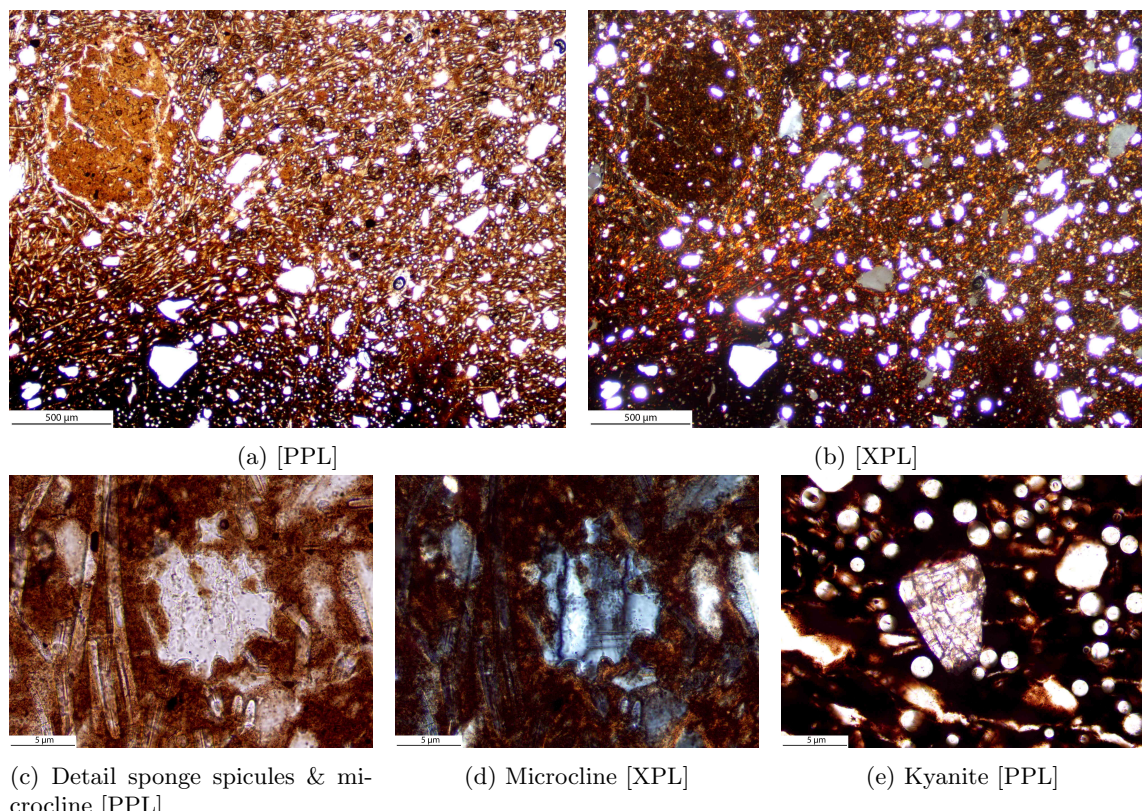


Figure S31

2.6 MUN 87/2-1-1-8:3 (mun#107; Fig. S9.4; Pikunda-Munda style; Seidensticker, 2021, 472 Pl. 91.7)

The samples non-calcareous fine fraction is two-tiered with undifferentiated b-fabric (very darkish brown [PPL]) at the center of the section and stipple-speckled b-fabric (yellowish brown [PPL]) at the exterior half and very narrowly at the interior part. The boundary between the zones is very acute (a–b). While voids are rare, they show an orientation that is predominantly diagonal in the plane of the section. The coarse

fraction is dominated by sponge spicules and sub-angular quartz in a unimodal grain-size distribution. Also present, but rare, are clay pellets (c–d), plagioclase (c–d), tourmaline and zircon. The c/f-related distribution pattern is single-spaced porphyric (single- to double-spaced porphyric if only quartz grains are regarded as coarse material).

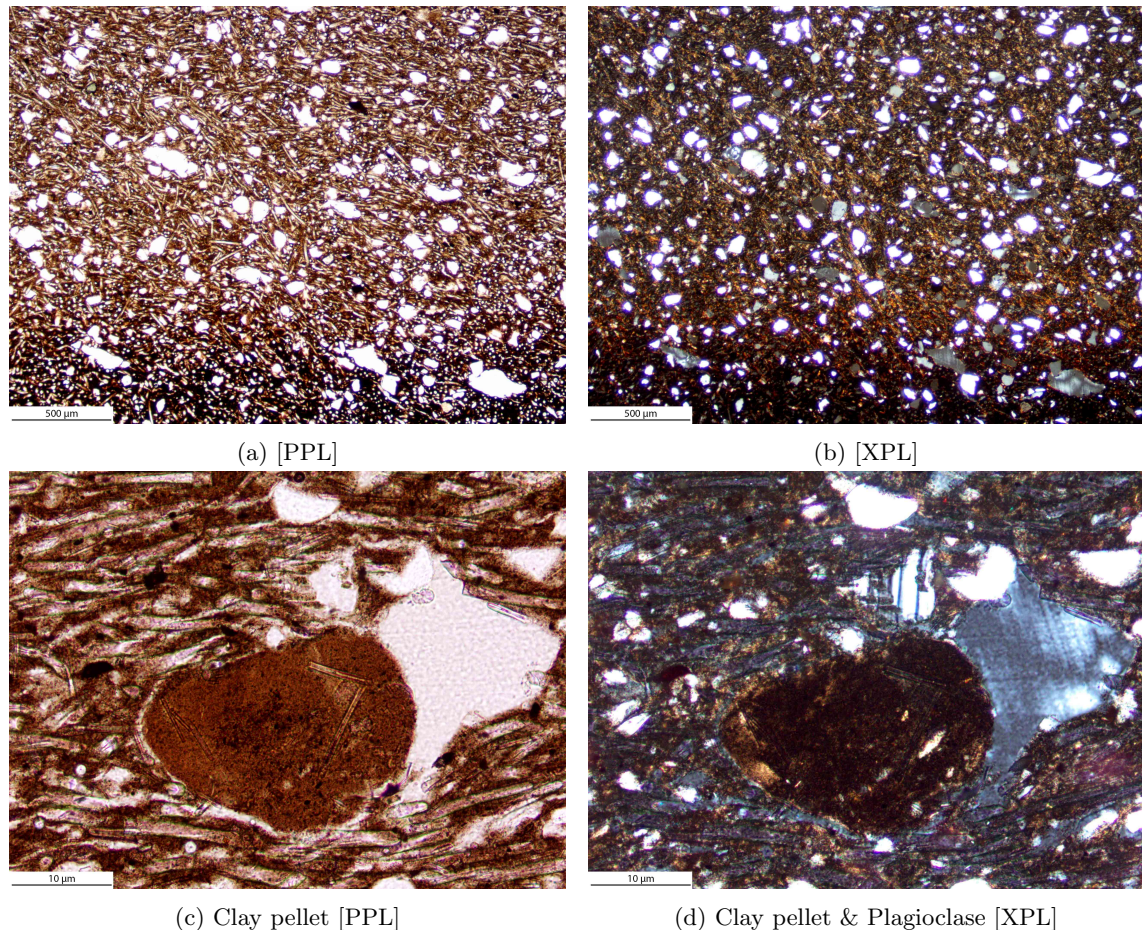


Figure S32

2.7 MUN 87/2-1-3-1:2 (mun#103; Fig. S9.7; Pikunda-Munda style; Seidensticker, 2021, 473 Pl. 92.2)

The samples non-calcareous fine fraction is homogeneous with undifferentiated b-fabric (very darkish brown [PPL]). Voids are narrow and run predominantly wall-parallel through the section. The coarse fractions main component are sponge spicules, showing zonation in terms of their orientation. There are alternating bands of spicules cut predominantly transversal or longitudinal in

relation to the plane of the section (a). The other dominating component of the coarse fraction is sub-angular quartz in a unimodal grain-size distribution. Rare are muscovite (c–f), staurolite (c–d), and tourmaline. The c/f-related distribution pattern is single-spaced porphyric (double-spaced to open porphyric if only quartz grains are regarded as coarse material).

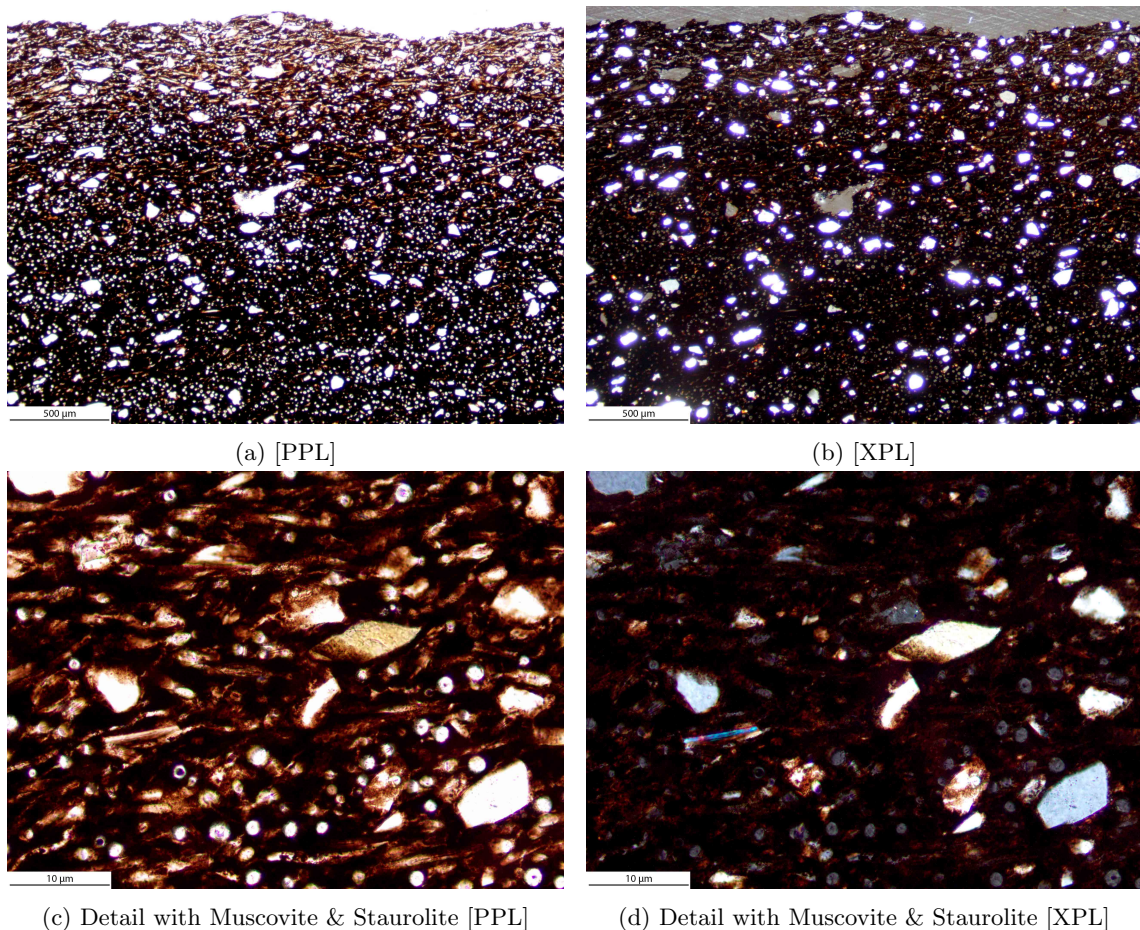


Figure S33

2.8 MUN 87/2-1-3-4:4 (mun#100; Fig. S9.8; Pikunda-Munda style; Seidensticker, 2021, 473 Pl. 92.4)

The sample shows a slightly heterogeneous non-calcareous fine fraction with a core with undifferentiated b-fabric (very darkish brown [PPL]) and with stipple-speckled b-fabric (darkish brown [PPL]) towards the exterior and interior surfaces of the sherd. This peripheral zone is very narrow and fades into the core (a). Very narrow voids that run predominantly diagonal in respect to the plane of the sherd, are frequent towards the exterior and interior surfaces. The

coarse fraction is dominated by sponge spicules. The spicules are predominantly cut transversal in relation to the plane of the section. The other dominating component of the coarse fraction is sub-angular quartz in a unimodal grain-size distribution. Very rarely present is zircon. The c/f-related distribution pattern is single-spaced porphyric (single- to double-spaced porphyric if only quartz grains are regarded as coarse material).

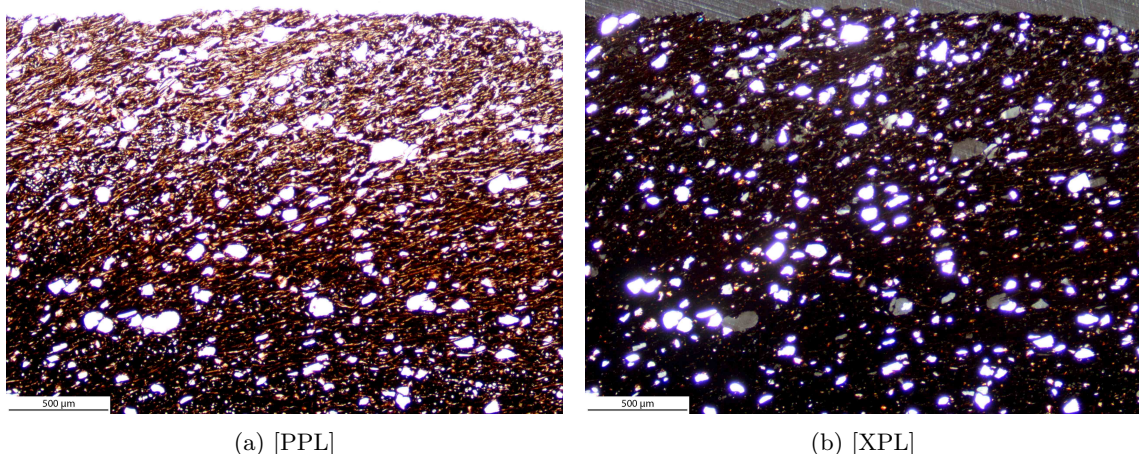


Figure S34

2.9 MUN 87/2-1-3:3 (mun#102; Fig. S9.9; Pikunda-Munda style; Seidensticker, 2021, 473 Pl. 92.5)

The samples non-calcareous fine fraction shows a distinct two-parted configuration: while with undifferentiated to slightly stipple-speckled b-fabric in both zones, the main body of the section is considerably dark (very darkish brown [PPL]), while the exterior shows a pale color (pale yellow [PPL]). The boundary between the two zones is strikingly sharp (a–b). Voids are rarely present and if so, very narrow. The section's coarse fraction is dominated by sponge

spicules. The spicules show a slight predominance of being longitudinally cut in relation of the plane of the section, opposed to transversal cut spicules. The other dominating component of the section's coarse fraction is sub-angular quartz in a unimodal grain-size distribution. Rare are muscovite, tourmaline, and staurolite. The c/f-related distribution pattern is single-spaced porphyric.

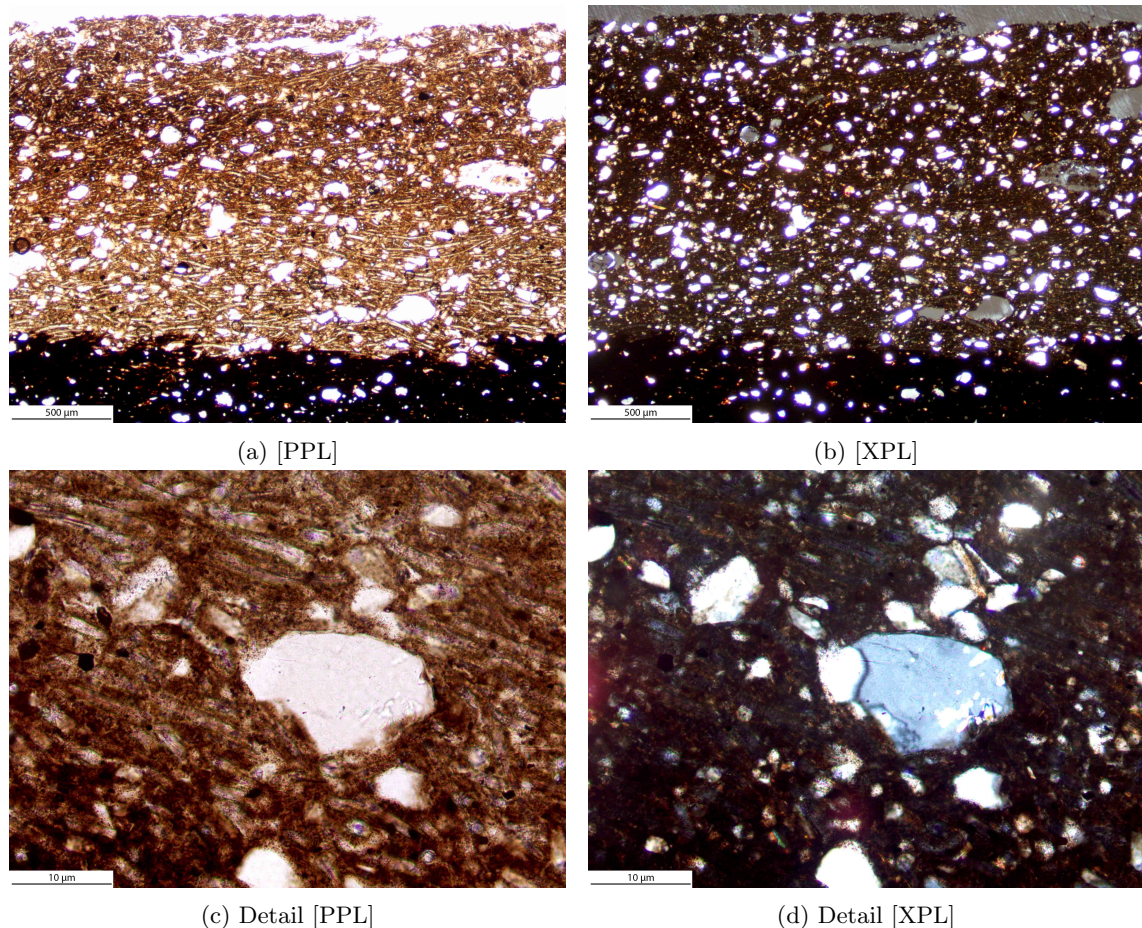
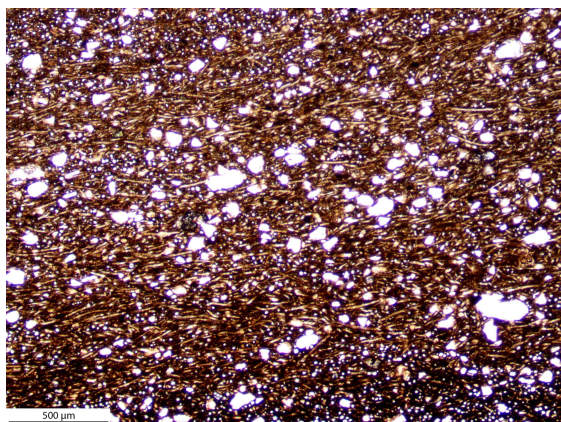


Figure S35

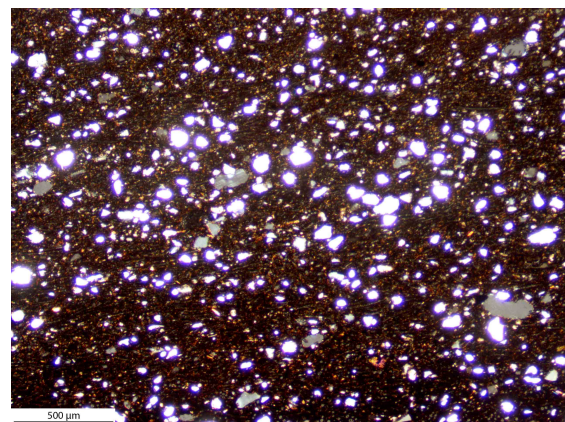
2.10 MUN 87/2-1-3:7 (mun#101; Fig. S9.10; Pikunda-Munda style; Seidensticker, 2021, 474 Pl. 93.1)

The sample shows a non-calcareous fine fraction with undifferentiated b-fabric in the center (dark brown [PPL]) and stipple-speckled b-fabric (brown [PPL]) towards the exterior and interior surfaces of the sherd. The boundaries between these two zones are blurry. Voids are very rare and narrow, if present. The coarse fraction is dominated by sponge spicules. The spicules are predominantly cut transversal in re-

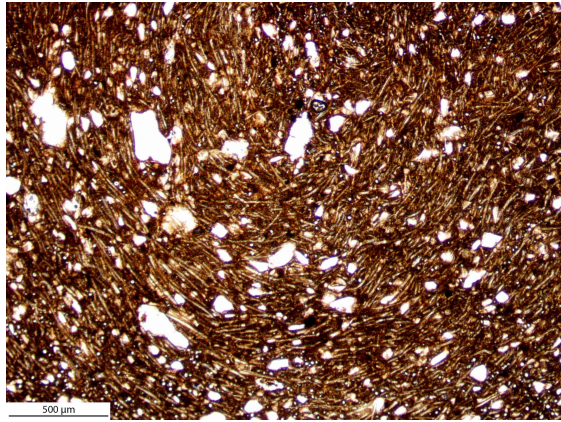
lation to the plane of the section. While the spicules are predominantly aligned parallel to the walls of the sherd (a), in one part, a concentric organization can be observed (c). The other dominating component of the section's coarse fraction is sub-angular quartz in a unimodal grain-size distribution. Rare are clay pellets, muscovite, and tourmaline. The c/f-related distribution pattern is single-spaced porphyric.



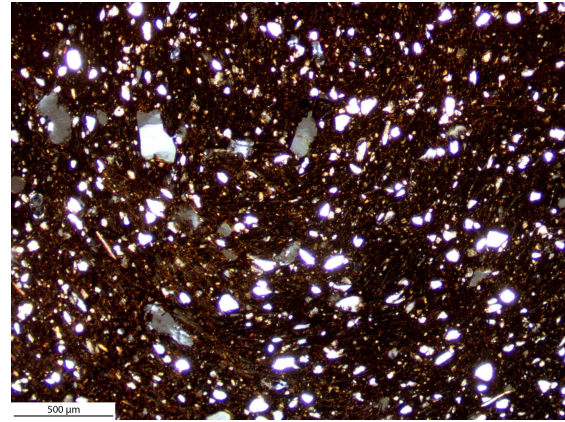
(a) Laminar organization of sponge spicules [PPL]



(b) [XPL]



(c) Concentric organization of sponge spicules [PPL]



(d) [XPL]

Figure S36

2.11 MUN 87/1-0-2-1:1 (mun#109; Fig. S9.12; Ebambe style; Seidensticker, 2021, 470 Pl. 89.4)

The sample's fine fraction is non-calcareous with stipple-speckled b-fabric, despite differences in coloration: while the interior section is dark (dark brown [PPL]), the exterior half is very lightly colored (yellowish brown [PPL]). The boundary between these two zones is blurry. Voids are very rare. The main component of the coarse fraction are sponge spicules. There is no clear pattern in spicules being cut transversal or

longitudinal in relation to the plane of the section. The second main component of the coarse fraction is fine quartz in a unimodal grain-size distribution. Rare are muscovite, staurolite, and zircon (c-d). The c/f-related distribution pattern is single-spaced porphyric (double-spaced to open porphyric if only quartz grains are regarded as coarse material).

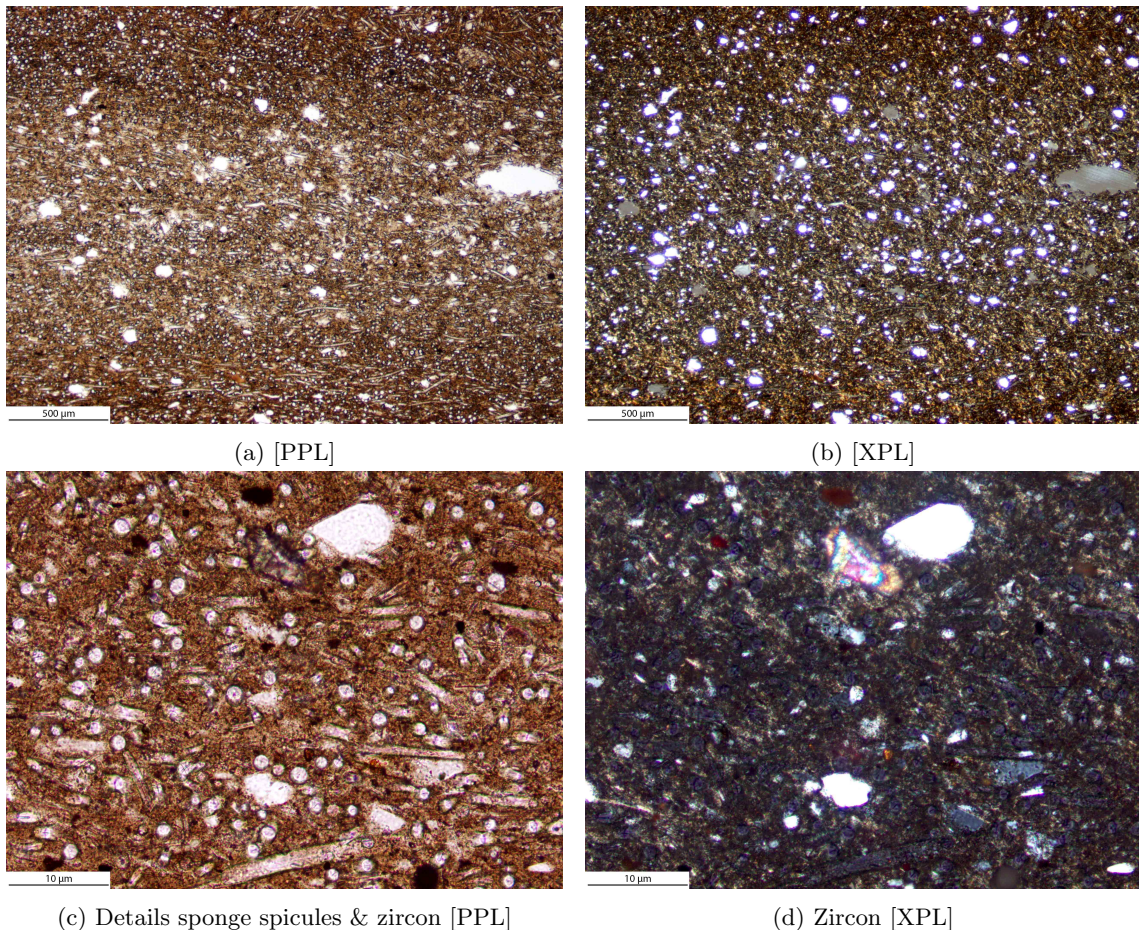


Figure S37

2.12 MUN 87/1-0-2-4:2 (mun#110; Fig. S9.11; Ebambe style; Seidensticker, 2021, 470 Pl. 89.2)

The sample shows a non-calcareous fine fraction with two zones: the core with undifferentiated b-fabric (dark brown [PPL]), while the parts of the sections corresponding to the exterior and interior of the sherd with stipple-speckled b-fabric (light yellow [PPL]). The boundary between these two zones is blurry. Voids are rare, and if they occur only narrow. The sam-

ple's coarse fraction consists mainly of sponge spicules and fine quartz in a unimodal grain-size distribution. Rare is muscovite, and very rare are zircon (c-d) and microcline (e-f). The c/f-related distribution pattern is single-spaced porphyric (single- to double-spaced porphyric if only quartz grains are regarded as coarse material).

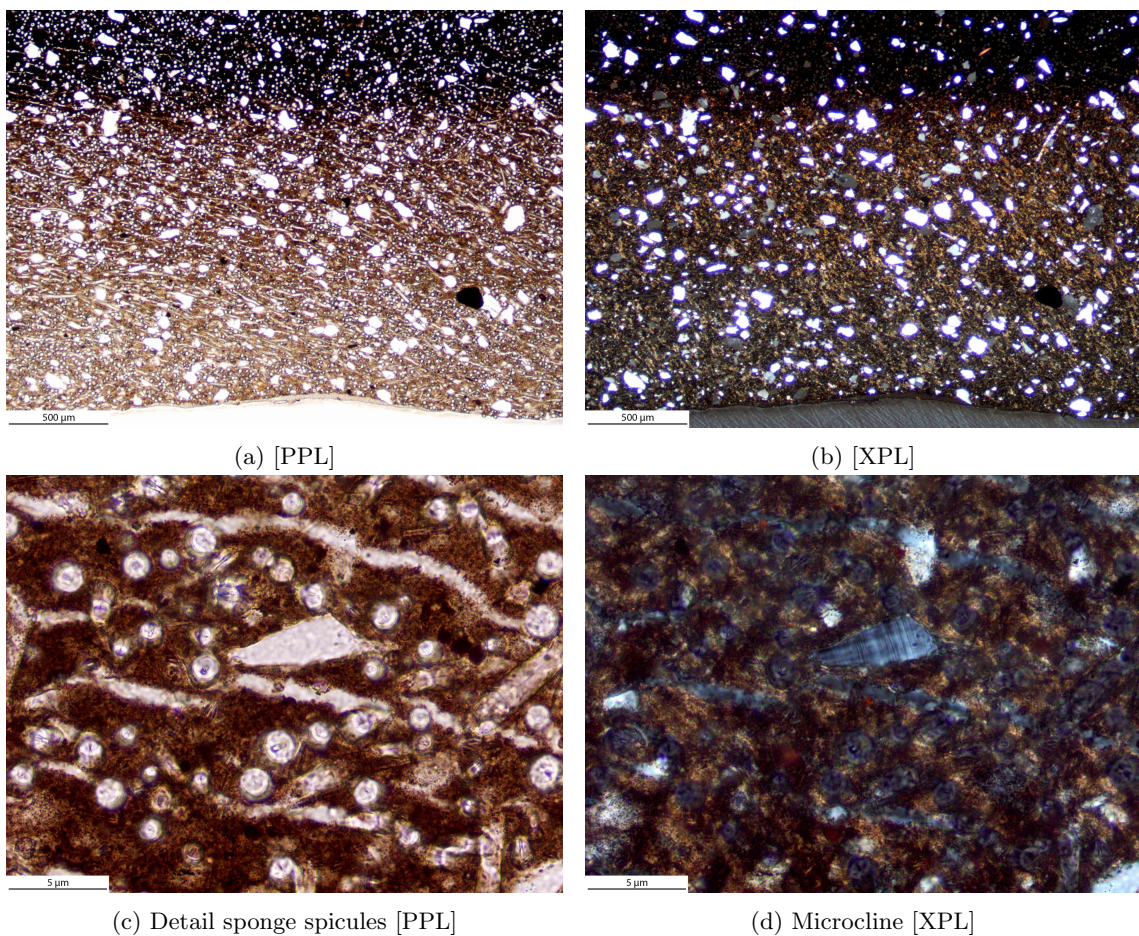


Figure S38

2.13 MUN 87/1-0-2-6:1 (mun#17; Fig. S9.14; Ebambe style; Seidensticker, 2021, 471 Pl. 90.2)

The sample shows a non-calcareous fine fraction in two zones: the interior with undifferentiated b-fabric (dark brown [PPL]) and the exterior half with stipple-speckled b-fabric (light yellow [PPL]). The boundary between these two zones is blurry. There are only very few, narrow voids. The coarse fraction's main component are sponge spicules and fine, sub-angular quartz in a unimodal grain-size distribution. In term of

the orientation of the spicules, where cut longitudinally in relation to the plane of the section, they are predominantly oriented diagonally, except for the exterior where concentric orientations occur (a). Very rare are biotite and tourmaline (d–e). The c/f-related distribution pattern is single-spaced porphyric (double-spaced to open porphyric if only quartz grains are regarded as coarse material).

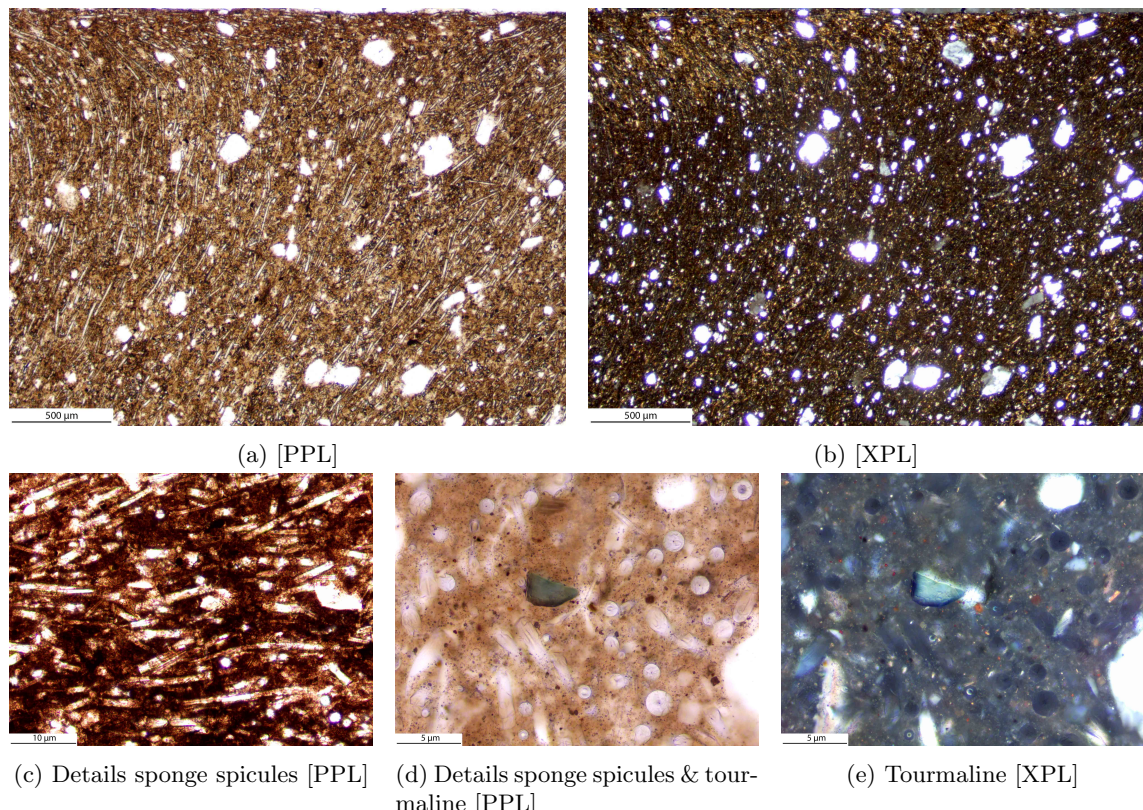


Figure S39

2.14 MUN 87/1-0-2-6:2 (mun#108; Fig. S9.13; Ebambe style; Seidensticker, 2021, 471 Pl. 90.1)

The sample's fine fraction (reddish brown [PPL]) is homogeneous and non-calcareous with stipple-speckled b-fabric. There are virtually no voids and the few that are present are very narrow. The coarse fraction's main component are sponge spicules and fine, sub-angular quartz in a unimodal grain-size distribution. In terms of the orientation of the spicules, there the areas in the section showing heterogeneity with certain

layers of spicules cut longitudinal in relation to the plane of the section, while in between those spicules are predominantly cut transversal (a, c, & e). Rare are muscovite and zircon (c-d). The c/f-related distribution pattern is single-spaced porphyric (double-spaced to open porphyric if only quartz grains are regarded as coarse material).

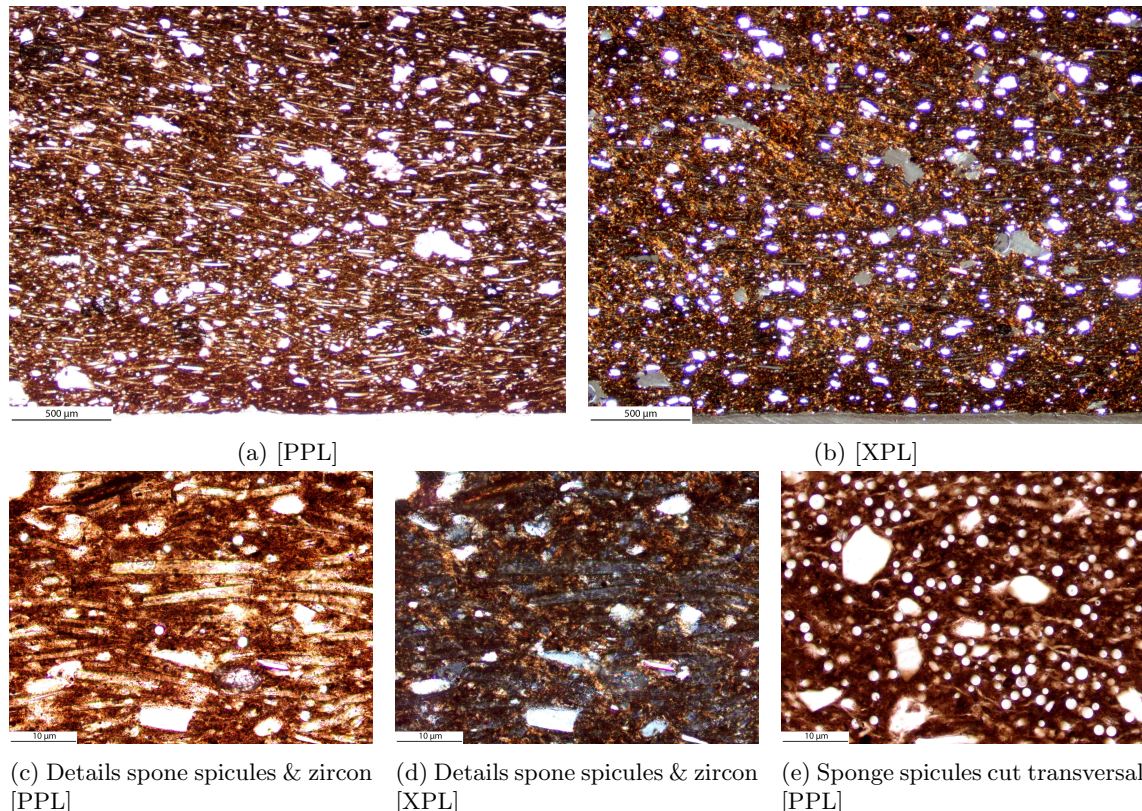


Figure S40

3 Wafanya

3.1 WAF 83/16-2:1 (waf#47; Fig. S12.2; Monkoto style; Wotzka, 1995, 504 Pl. 70.10)

The fine fraction (yellowish brown [PPL]) is homogeneous and non-calcareous with unistriated b-fabric. Voids are diagonally oriented. The main component of the coarse fraction are sponge spicules, while sub-angular quartz is less frequent. The quartz fraction shows a unimodal

grain-size distribution. Charred plant matter (e–g), staurolite (c–d) and tourmaline are rarely present. The c/f-related distribution pattern is single-spaced porphyric (open porphyric if only quartz grains are regarded as coarse material).

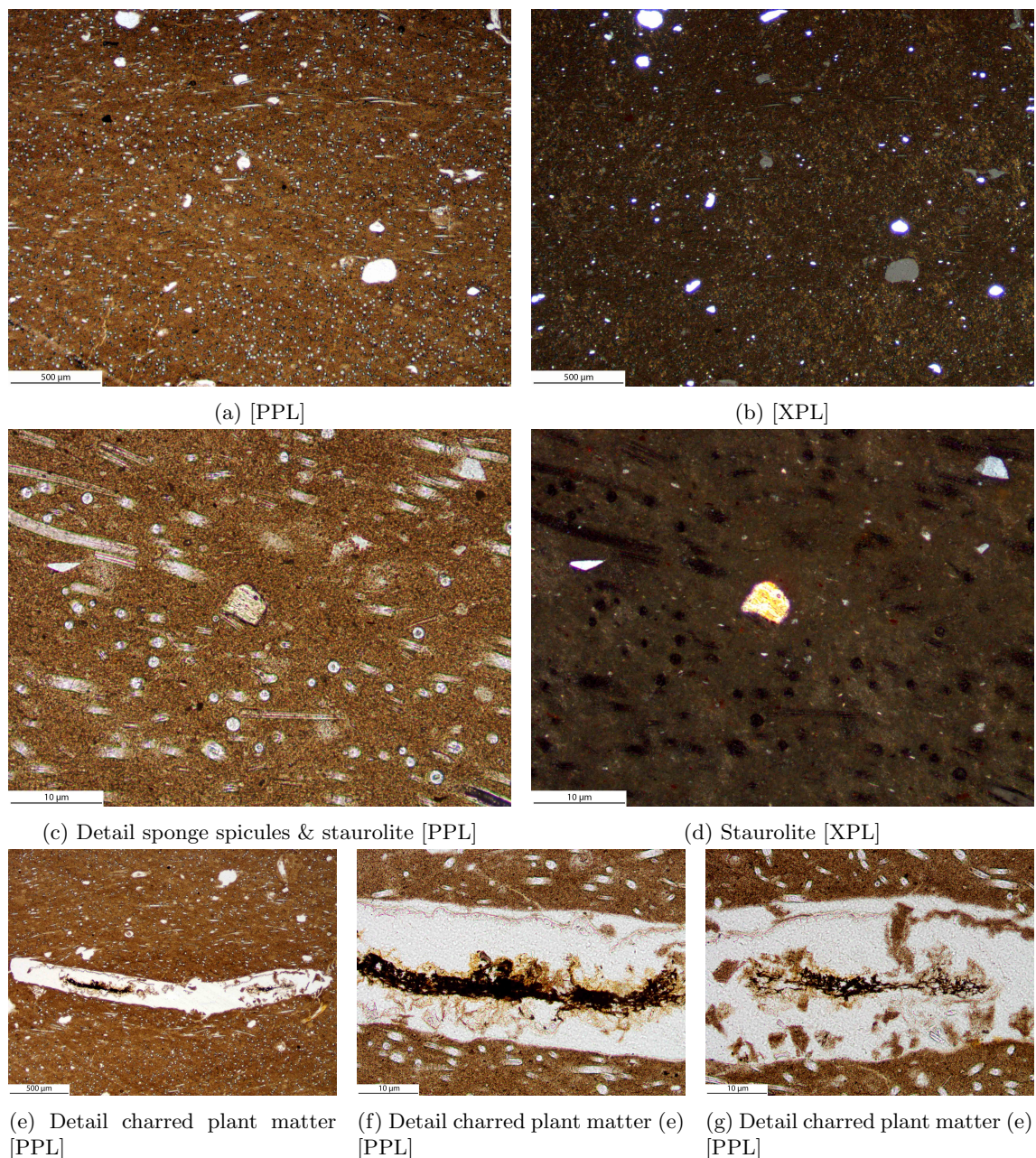


Figure S41

3.2 WAF 83/16-2:3 (waf#48; Fig. S12.6; 3K–L; Bekongo style; Wotzka, 1995, 503 Pl. 69.6)

The sample's fine fraction is homogeneous and non-calcareous (yellowish-brown [PPL]) with stipple-speckled b-fabric. Voids are numerous and often filled with remnant of charred plant matter (a). Remnants of the parenchyma of Poaceae could be identified (c-d). The main component of the coarse fraction is sub-angular

quartz, which is present in a bimodal grain-size distribution. Less frequent are muscovite, while tourmaline and microcline are rare. Also rare are rock fragments (metamorphic) (e). The c/f-related distribution pattern is single-spaced porphyric.

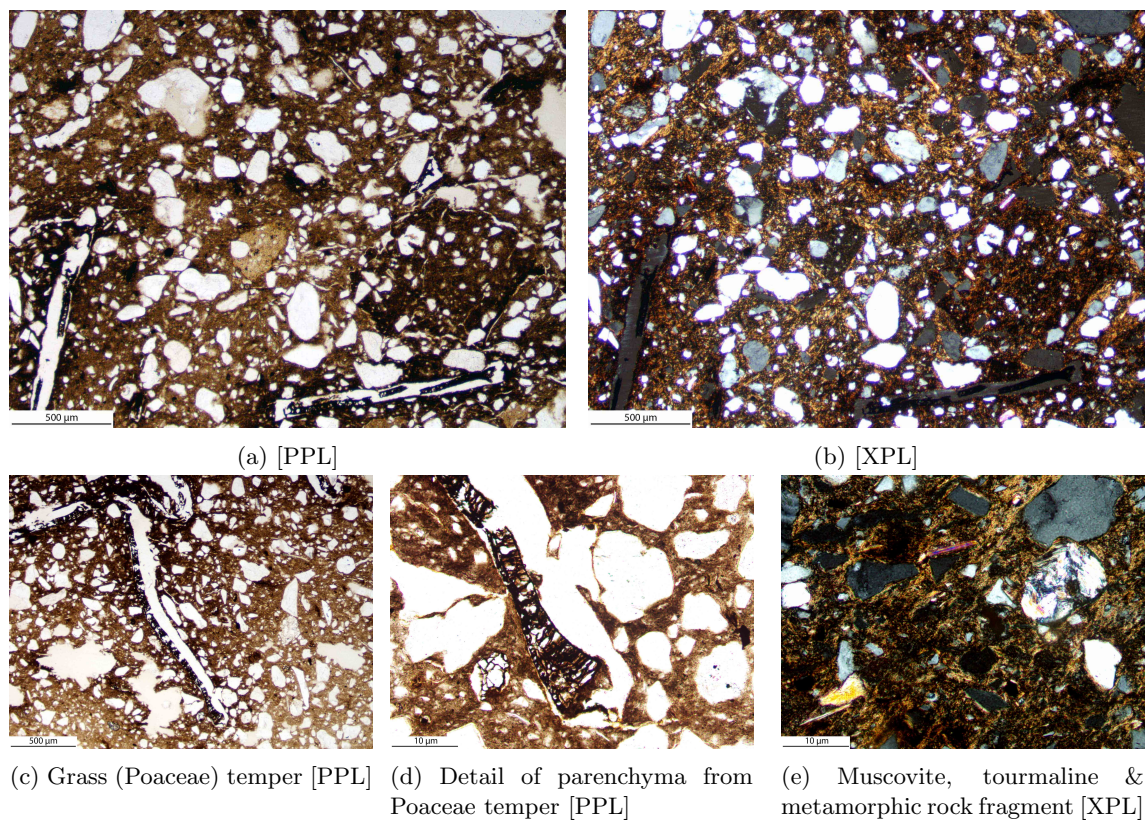


Figure S42

3.3 WAF 83/16-5:33 (waf#96; Fig. S12.5; Bekongo style; Wotzka, 1995, 503 Pl. 69.5)

The sample's fine fraction is homogeneous and non-calcareous (reddish-brown [PPL]) with stipple-speckled b-fabric. Voids are present and often filled with remnants of charred plant matter (c-d). The main component of the coarse

fraction is sub-angular quartz in a unimodal grain-size distribution. Less frequent are muscovite, while staurolite (f-g) and zircon (h-i) are rare. The c/f-related distribution pattern is single-spaced porphyric.

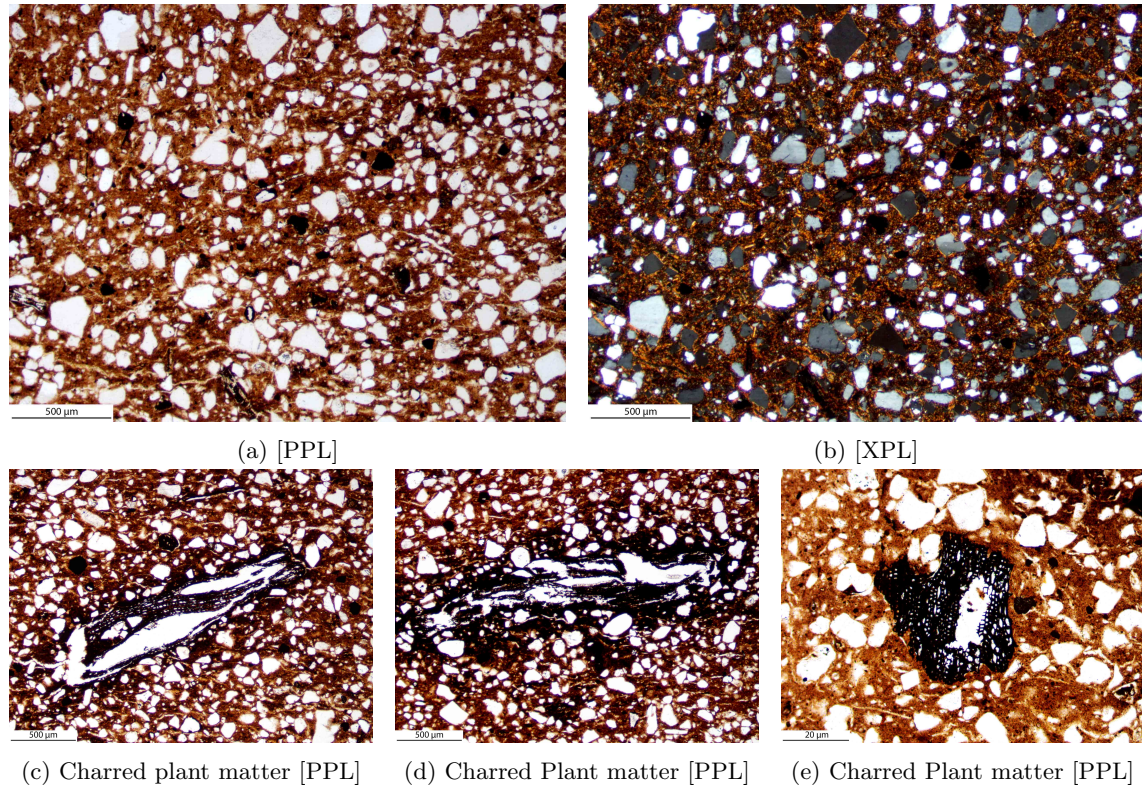


Figure S43

3.4 WAF 83/16-7-1:2 (waf#49; Fig. S12.7; Longa style; Wotzka, 1995, 503 Pl. 69.9)

The samples non-calcareous fine fraction is very homogeneous (light yellow [PPL]) with stipple-speckled b-fabric (localized unistriation). The section shows no voids. The coarse fraction is dominated by sponge spicules and sub-angular quartz. The quartz fraction shows a unimodal

grain-size distribution. Part of the quartz fraction consists of runiquartz, while some grains show rolling extinction (b). Also frequent are iron rich clay pellets (a). Rare are biotite, tourmaline and zircon. The c/f-related distribution pattern is single-spaced porphyric.

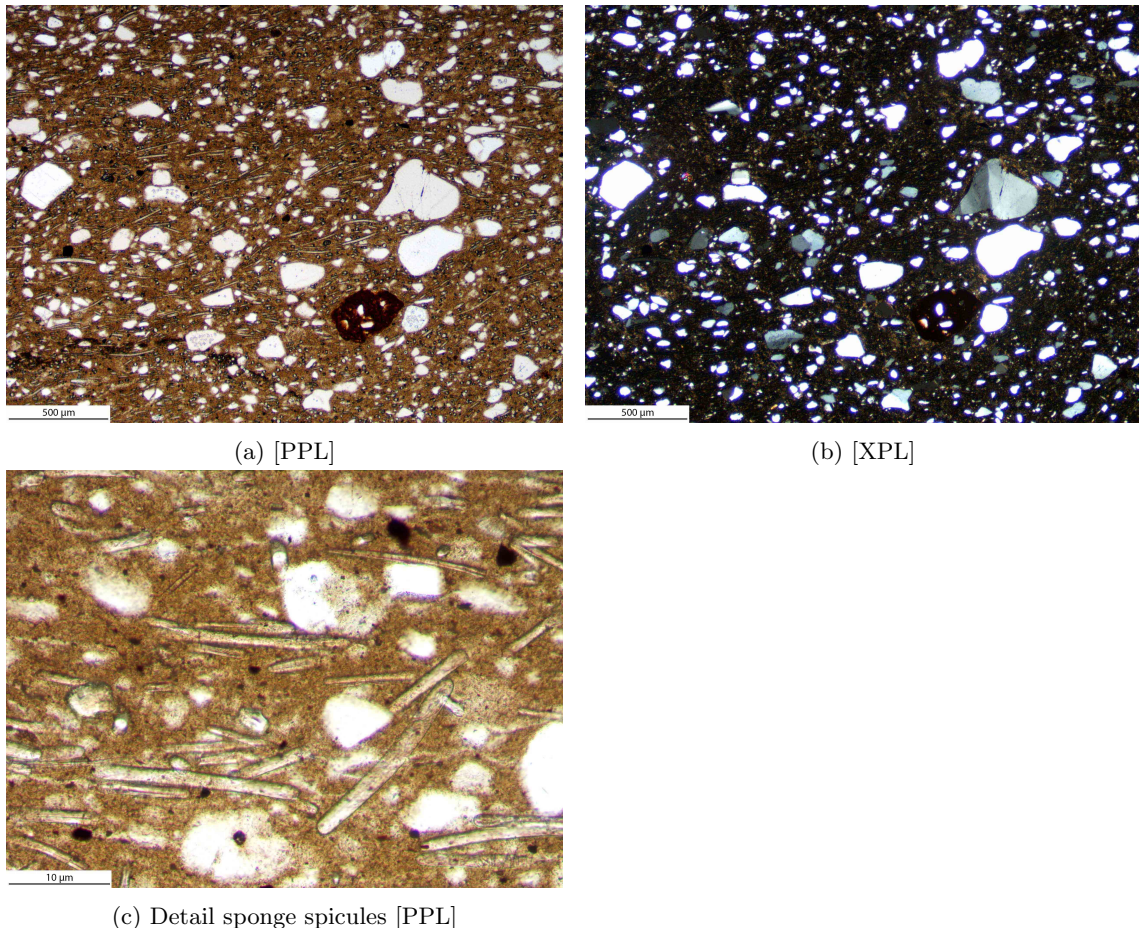


Figure S44

4 Salonga National Park

4.1 SNP 01 7:1 (snp#43, Fig. S11.1; cf. Bokuma style)

The samples fine fraction (light yellow to dark brown [PPL]) is non-calcareous with unistriated b-fabric. Voids are narrow and predominantly oriented wall-parallel. The main component of the coarse fraction are sponge spicules. Subangular quartz in a unimodal grain-sizes distri-

bution is also present. Rare are charred plant matter (c), zircon and staurolite. The c/f-related distribution pattern is single-spaced porphyric (open porphyric if only quartz grains are regarded as coarse material).

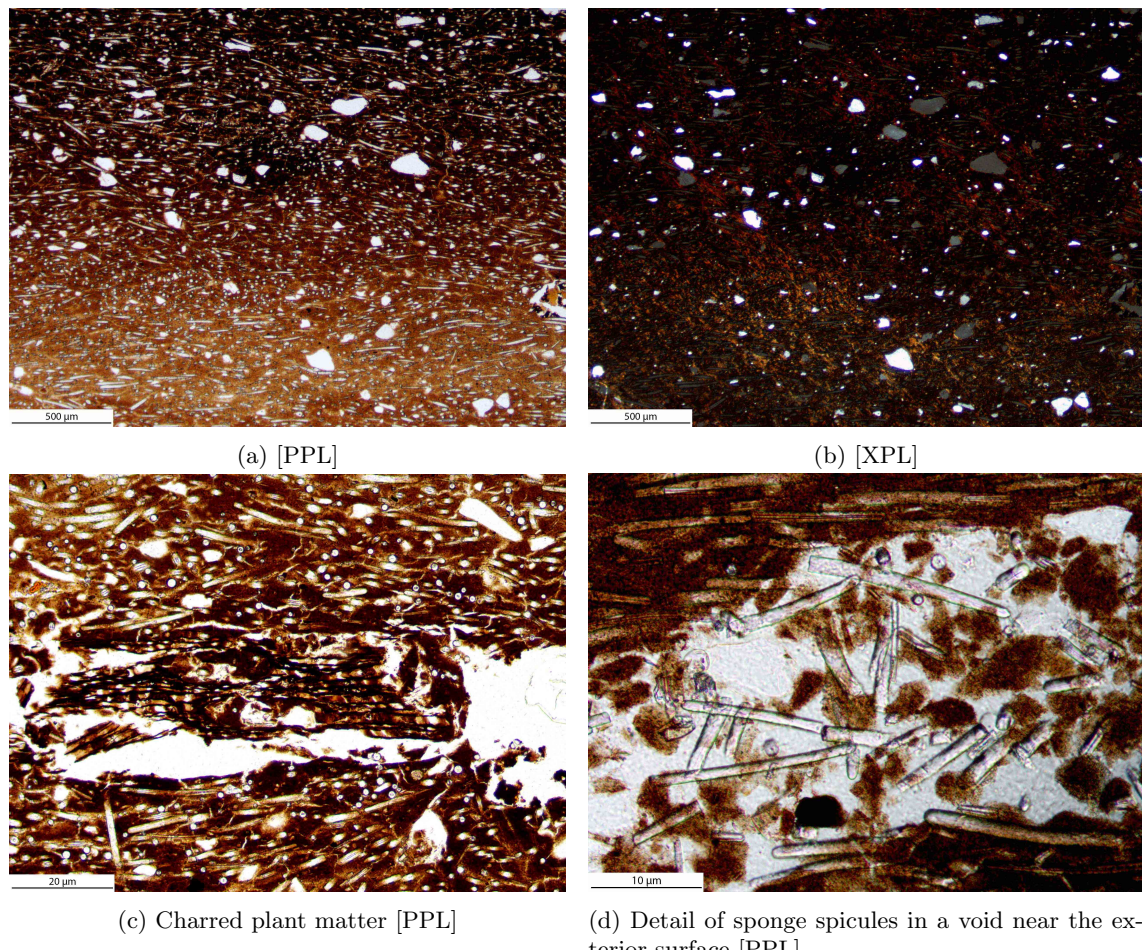


Figure S45

4.2 SNP 03-4:1 (snp#42; Fig. 3G–H; S11.5)

The non-calcareous fine fraction of the sample (light yellow to slightly reddish brown [PPL]) is homogeneous and non-calcareous with stipple-speckled b-fabric (localized granostriation). Voids are frequent and oriented wall-parallel or at the edges of constituents of the coarse fraction. The main components of the coarse fraction are sub-angular quartz and an-

gular grog particles. Some of the quartz grains show rolling extinction. The grog shows a similar composition as the fine fraction of the sherd itself, only their colors are more intense brownish and reddish [PPL]. Grain-sizes within the coarse fraction are distributed bimodal. Rare are muscovite and zircon. The c/f-related distribution pattern is double-spaced porphyric.

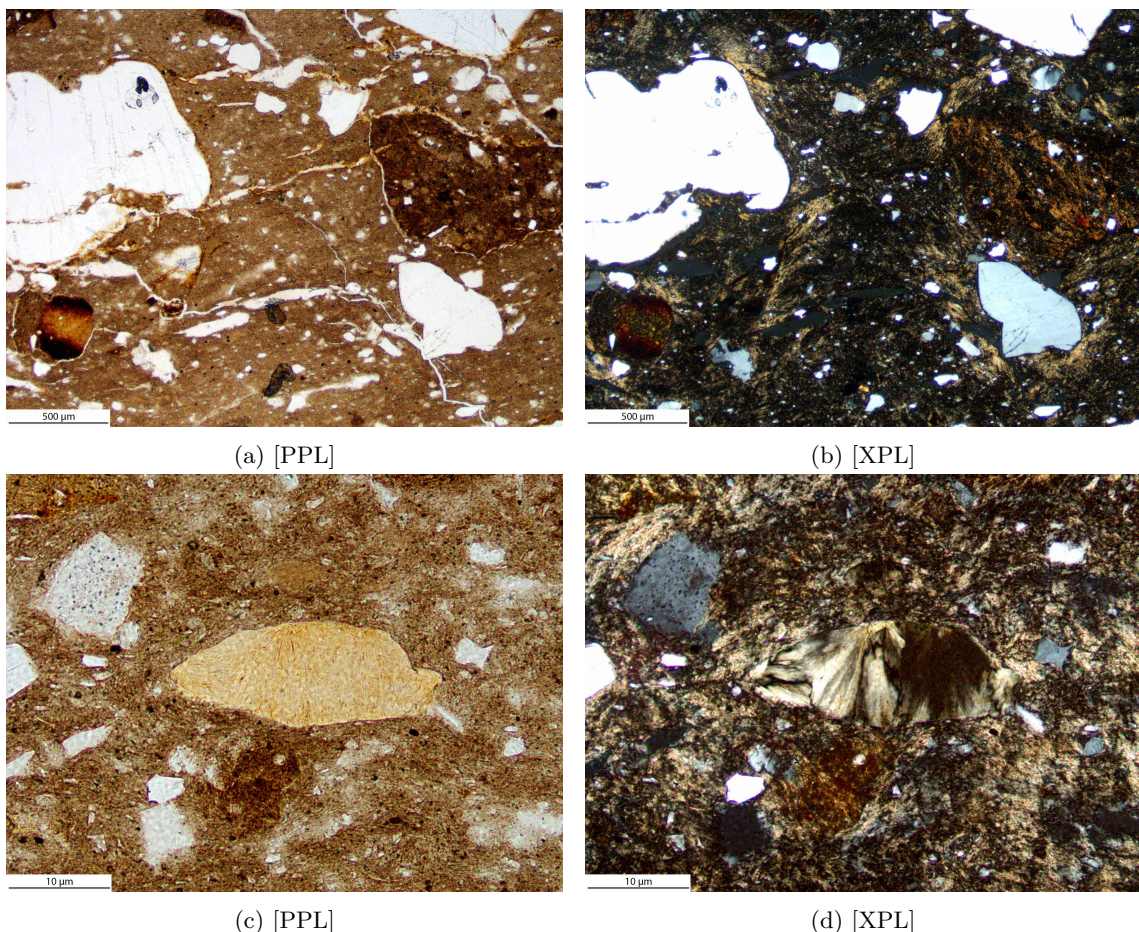


Figure S46

4.3 SNP 03-4:4 (snp#45)

The samples fine fraction (light yellow [PPL]) is non-calcareous with stipple-speckled b-fabric (localized cross-striation). Voids are predominantly wall-parallel oriented. The main component of the coarse fraction are sub-angular quartz and angular grog particles. The grog

particles occasionally contain charred plant matter (d). The sample also contains homogeneous clay pellets with brighter brown to orange colors [PPL]. Occasionally muscovite is also present. The c/f-related distribution pattern is single-spaced porphyric.

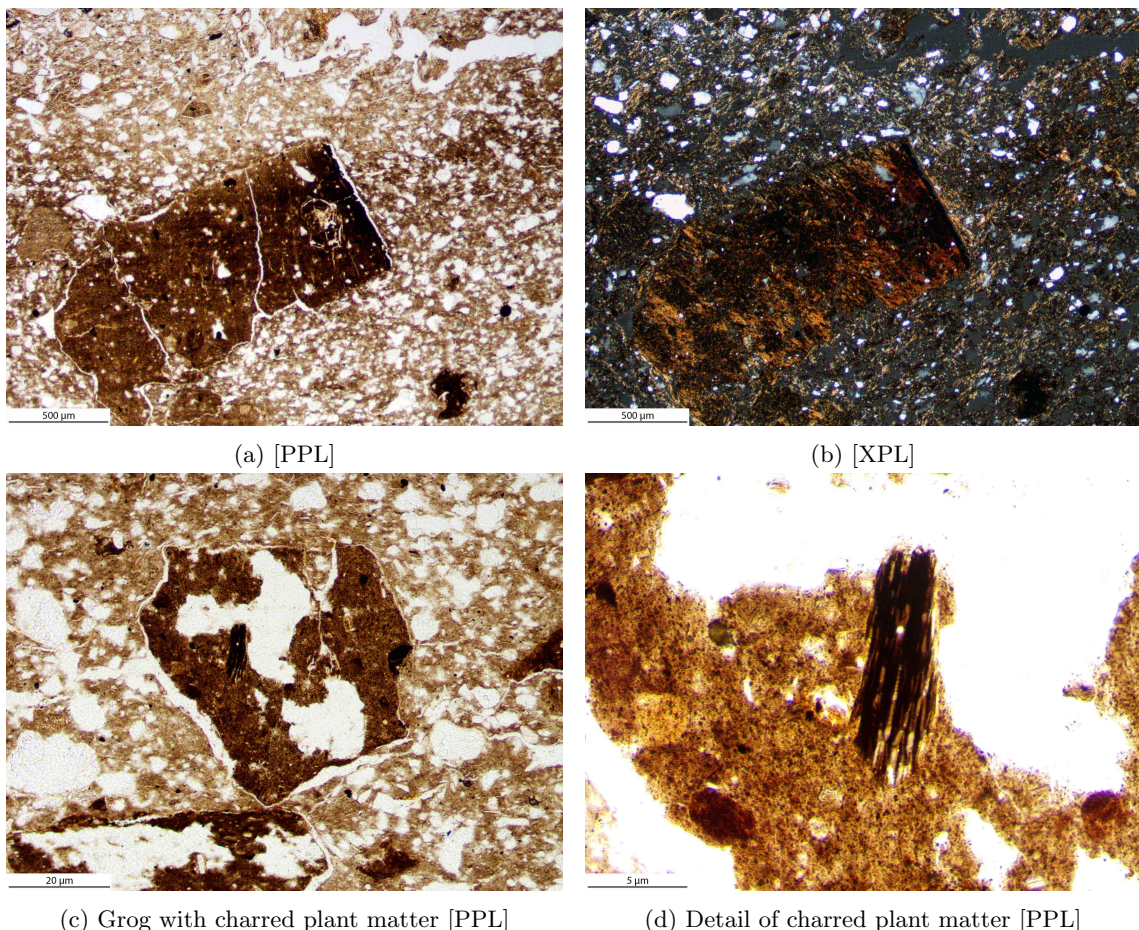


Figure S47

4.4 SNP 03-4:5 (snp#46; Fig. 3E–F)

The fine fraction (dark yellowish brown[PPL]) is non-calcareous with stipple-speckled b-fabric. The sample is streaked with voids, mostly in wall parallel orientation and around the components of the coarse fraction. The main constituents of the coarse fraction are sub-angular quartz in a bimodal grain size distribution and grog particles. The quartz fraction is partially composed of runiquartz. The fine fraction of the

grog particles is more intensely colored (brownish to orange-reddish [PPL]) than the fine fraction of the sherd itself. Secondary grog is frequent and zircon is more prevalent in the grog particles than in the main body. The sample also contains homogeneous clay pellets (reddish brown [PPL]), while muscovite and staurolite are rare. The c/f-related distribution pattern is single-spaced porphyric.

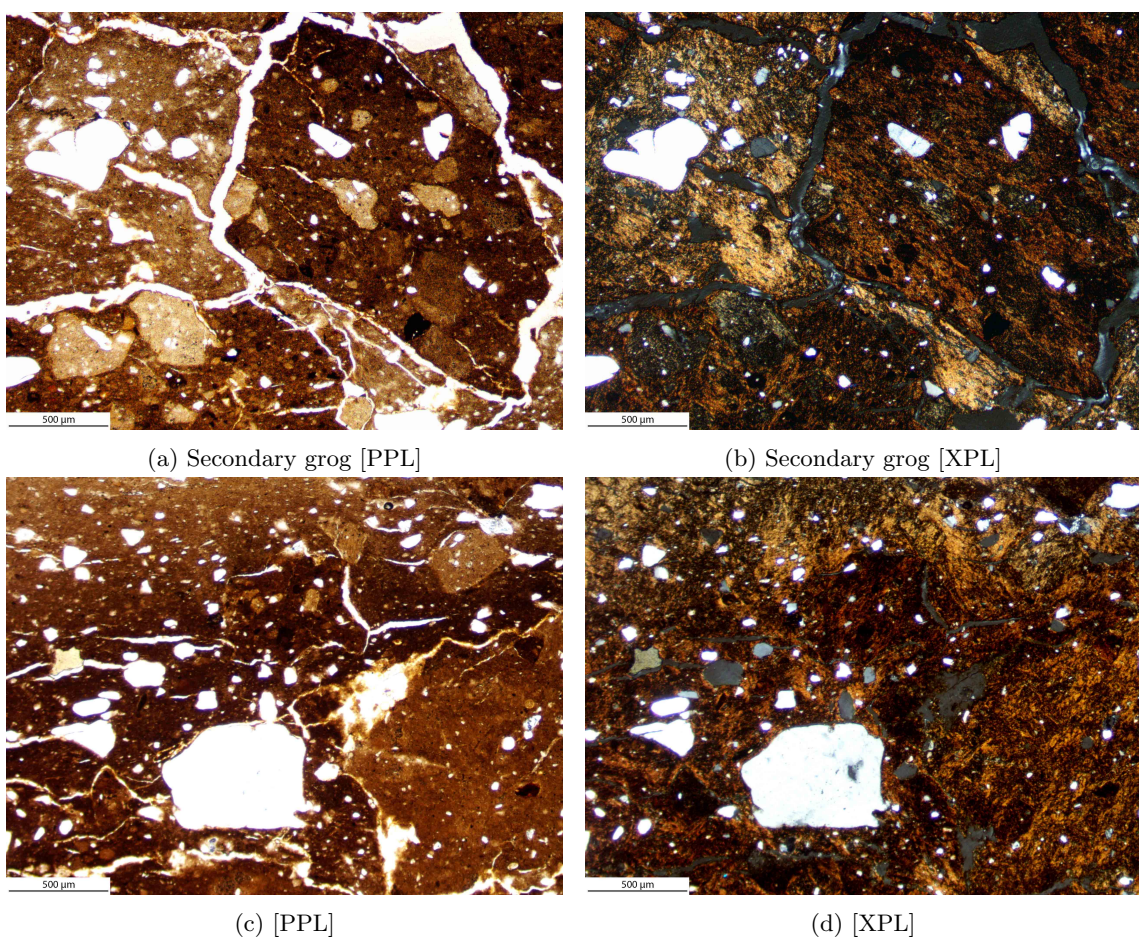


Figure S48

4.5 SNP 03-7:1 (snp#44; Fig. 3I; S11.7)

The sample shows a non-calcareous fine fraction (light yellowish brown [PPL]) with stipple-speckled b-fabric. Voids are narrow and mostly encompass the grog particles, a main component of the coarse fraction. Some voids contain remnants of charred plant matter (a). The angular grog particles are the main component of the coarse fraction. The fine fraction of them is often more intensely colored (reddish dark brown [PPL]) than the fine fraction of the main body.

Some grog particles show secondary grog and sub-angular quartz in a bimodal grain size distribution. The main body also contains sub-angular quartz in a unimodal grain-sizes distribution. Rare are homogenous clay pellets (bright yellow [PPL]) and dense lumps of quartz particles (soil deposits) (c-d). Muscovite and biotite are rare. The c/f-related distribution pattern is single-spaced porphyric.

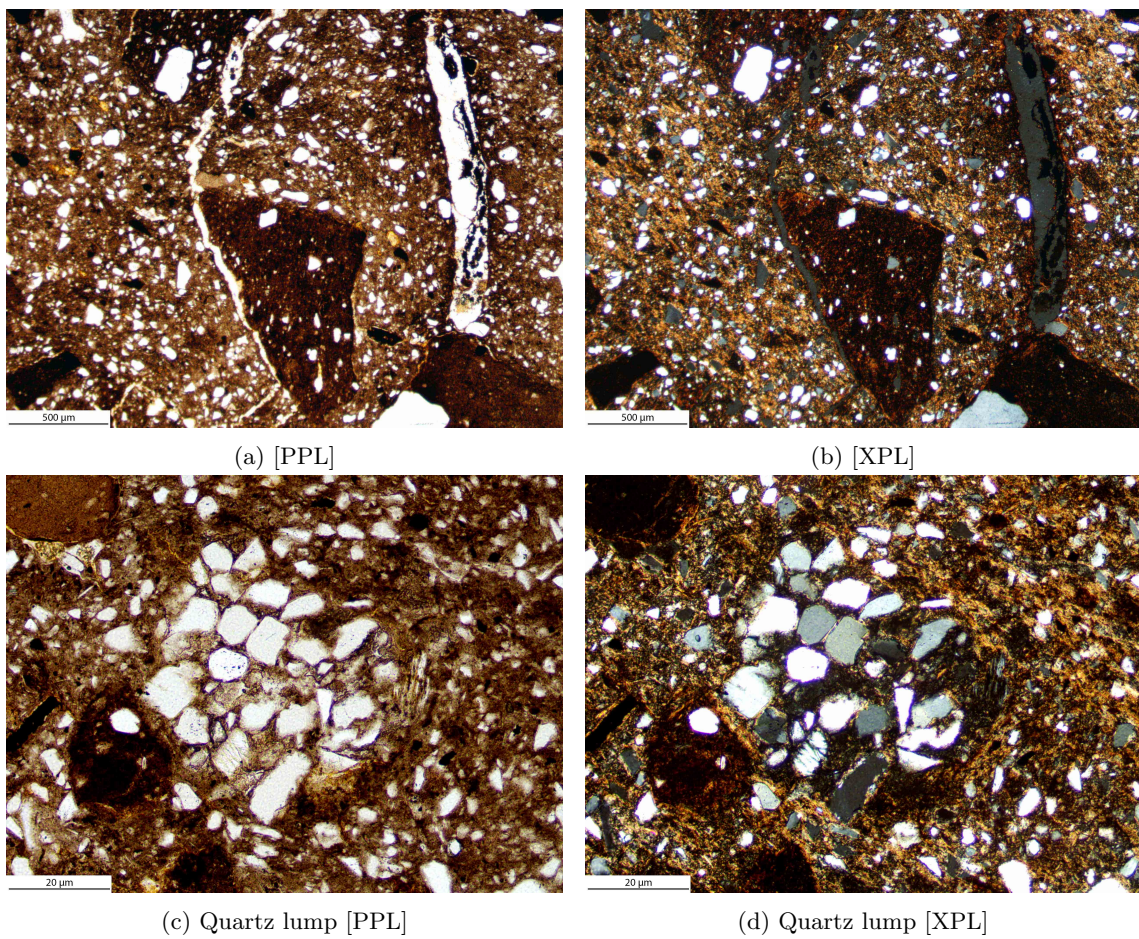


Figure S49

5 Monkoto

5.1 MON 83/101:1 (mon#50; Fig. S12.1; Monkoto style; Wotzka, 1995, 506 Pl. 72.5)

The samples fine fraction is homogeneous and non-calcareous (yellowish brown [PPL]) with unistriated b-fabric. Voids are rare and very narrow. The main component of the coarse fraction is sub-angular quartz in a unimodal grain-size distribution, partially showing rolling ex-

tinction. Also present are sponge spicules, homogenous clay pellets (reddish brown [PPL]) and grog particles rich in sponge spicules. Biotite and tourmaline are rare. The c/f-related distribution pattern is single-spaced porphyric.

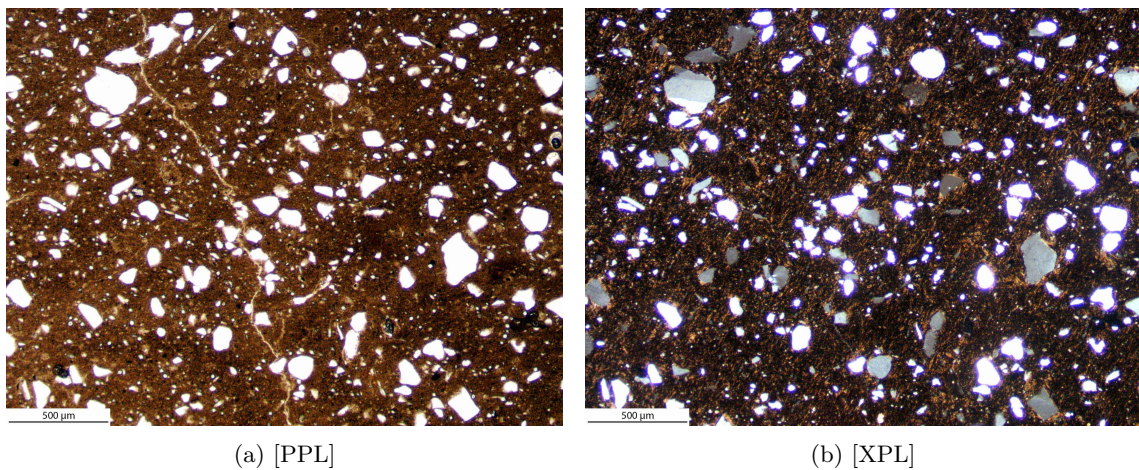


Figure S50

5.2 MON 83/101:3 (mon#51; Fig. S12.3; 3D; Monkoto style; Wotzka, 1995, 506 Pl. 72.6)

The sample shows a homogeneous non-calcareous fine fraction (light yellow to dark reddish brown [PPL]) with undifferentiated b-fabric. Voids are rare and narrow, they usually encompass grog particles. The main component of the coarse fraction is sub-angular quartz in a unimodal grain-size distribution. Also frequent are grog particles (fine fraction:

light yellow [PPL]) rich in sponge spicules and sub-angular quartz. Less frequent are sponge spicules, homogenous clay pellets (red-brown [PPL]), charred plant matter and zircon. One void shows the remnant of a charred plant seed (c). Tourmaline and muscovite are rare. The c/f-related distribution pattern is single-spaced porphyric.

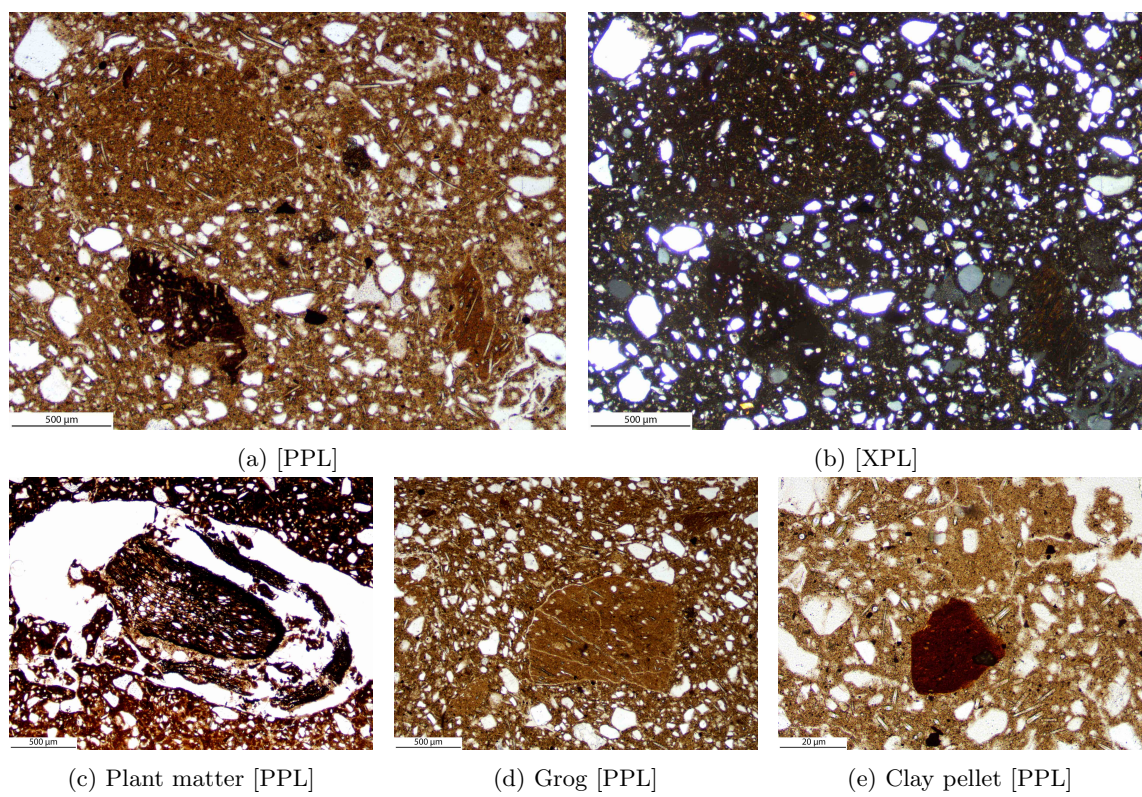


Figure S51

5.3 MON 83/101:4 (mon#52; Fig. S12.4; 3J; Wotzka, 1995, 505 Pl. 71.6)

The samples fine fraction is homogeneous and non-calcareous (dark brown [PPL]) with undifferentiated b-fabric. Voids are present, without them showing any predominant orientation. The main component of the coarse fraction are densely packed sub-angular quartz in a slightly bimodal grain-size distribution. Also very prominent is charred plant matter and grog

particles. While one void contains remnants of a plant seed (a), others contain plant matter reminiscent of parenchyma. While the fine fraction of the main body shows very few sponge spicules (d), the grog component regularly is derived of fired clays rich in sponge spicules (a). Rare are muscovite and staurolite. The c/f-related distribution pattern is single-spaced porphyric.

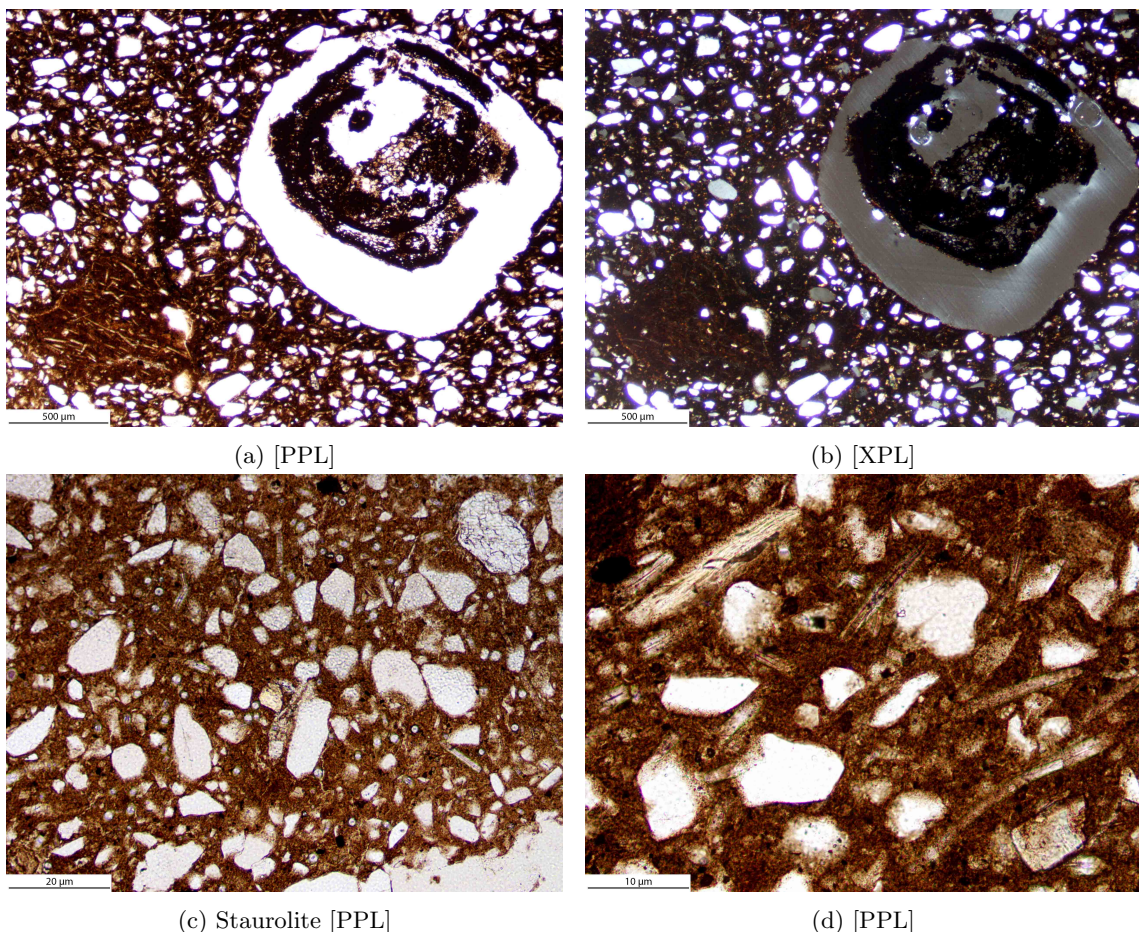


Figure S52

References

- W. S. MacKenzie, A. E. Adams, and K. H. Brodie. *Rocks and Minerals in Thin Section*. CRC press, Boca Raton, revised 2nd ed edition, 2017. ISBN 978-1-138-02806-7 978-1-138-09184-9 978-1-315-11636-5.
- P. S. Quinn. *Thin Section Petrography, Geochemistry and Scanning Electron Microscopy of Archaeological Ceramics*. Archaeopress Archaeology, Oxford, 2 edition, 2022. ISBN 978-1-80327-271-9.
- D. Seidensticker. *Archäologische Untersuchungen zur eisenzeitlichen Besiedlungsgeschichte des nordwestlichen Kongobeckens*. Tübingen University Press, Tübingen, Sept. 2021. ISBN 978-3-947251-48-3.
- G. Stoops. *Guidelines for Analysis and Description of Regolith Thin Sections*. ASA, CSSA, and SSSA Books. Wiley-ACSESS, Hoboken, NJ, second edition edition, 2021. ISBN 978-0-89118-975-6.
- H.-P. Wotzka. *Studien zur Archäologie des zentralafrikanischen Regenwaldes: Die Keramik des inneren Zaire-Beckens und ihre Stellung im Kontext der Bantu-Expansion*, volume 6 of *Africa Praehistorica*. Heinrich-Barth-Institut, Köln, 1995. ISBN 3-927688-07-X.